University of London

Imperial College of Science and Technology

Department of Physics

Applied Optics Section

"A Form of Three-beam Interferometer Of High Sensitivity"

A Thesis Submitted For The Degree

Of

Doctor of Philosophy

By

Manohar Lal Soni

November, 1968.

Contents

Abstract

In the past three-beam interferometers have taken the form of analogues of the Rayleigh two-beam interferometer. The present work was undertaken with a two-fold aim. The first was to make a detailed study of the permissible tolerances on the relative orientations of the three waves and of the influence of differences in amplitude between them: the second was to design and construct a three-beam analogue of the Michelson interferometer and to study the possibilities of photo-electric detection.

Three-beam interference is usually considered as the coherent superposition of a third wavefront on the two-beam fringes formed by the other two. The third wavefront has then to be parallel to the bisecting plane of the other two waves if uniform fringes are to be obtained. Formulae for the tolerances on this setting have been obtained. The amplitude of the third wave, relative to that of the other two, can be chosen to optimise the signal/noise ratio if photo-electric detection is employed. Formulae for this purpose have been studied. An important finding was that even a small inequality of amplitude of the waves forming the two-beam background fringes leads to significant asymmetry of the three-beam fringes. This last requirement could only be met in the Rayleigh form by imposing impractically severe tolerances on equality of width of the two slits.

The new instrument was designed in the general form of a Michelson interferometer. The reflecting system in one arm has a glass cube interferometer in which the resulting two beams both undergo a reflection and transmission. In this way, equality of amplitude for the two-beam fringes was more easily ensured. The mechanical design of the apparatus unfortunately did not permit the extreme degree of stability demanded by the great sensitivity of the fringes. The form of the three-beam fringes was also found to be highly sensitive to errors of flatness of the third wave. For these reasons, and shortage of time, only a preliminary experimental study of the problem was possible.

CHAPTER I

Introduction:

In a two beam interferometer two coherent beams of light are arranged to combine in such a way that reinforcement and cancellation of the illumination takes place at different points, depending on the phase differences of the two beams. Also the light emitted by all elements of the source must form identical fringe patterns in which the maxima fall in the same place, otherwise the various patterns may overlap maxima and minima and result in reduced, or even zero, contrast. When the above mentioned conditions are satisfied the two beams are said to be "spatially coherent".

The basic system of an interferometer can be shown by a block diagram, Fig. 1. The way in which two beams are split-off from the primary beam constitutes a possible basis for the classification of a two-beam interferometer. The main methods are:-

a) Aperture-splitting

b) Diffraction-splitting

c) Amplitude-splitting

We consider the first one. A good example of this is met in Rayleigh's interferometer, whose arrangement is shown by Fig. 2(a).

Light from a vertical slit source S_1 is collimated by a lens L_1 which falls on a screen pierced by two slits, S_2 and S_3 and then passes through the tubes T_1 and T_2. The light is brought to focus again by another lens L_2, when fringes are formed in its focal plane,

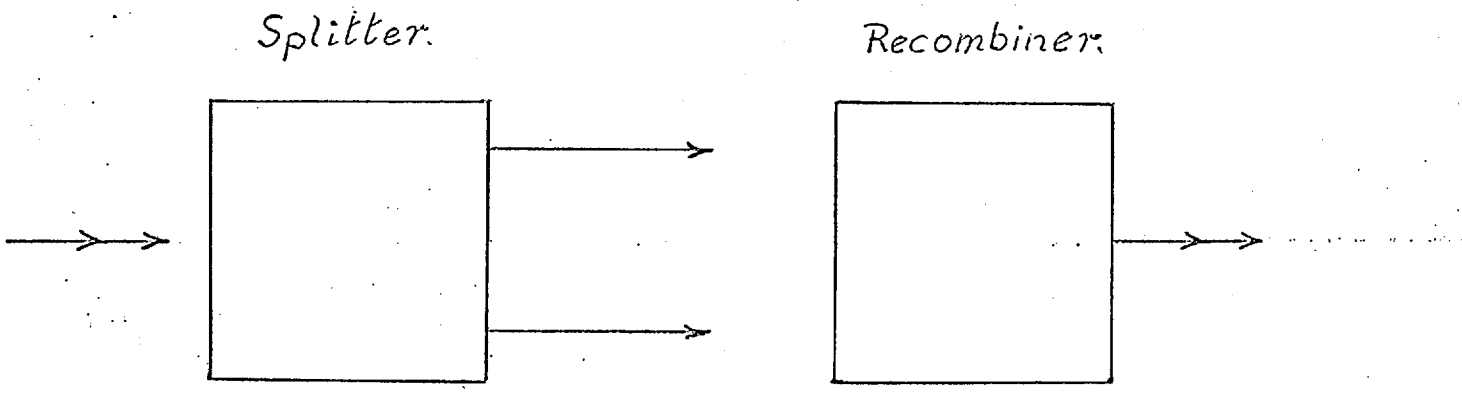

Fig. 1.

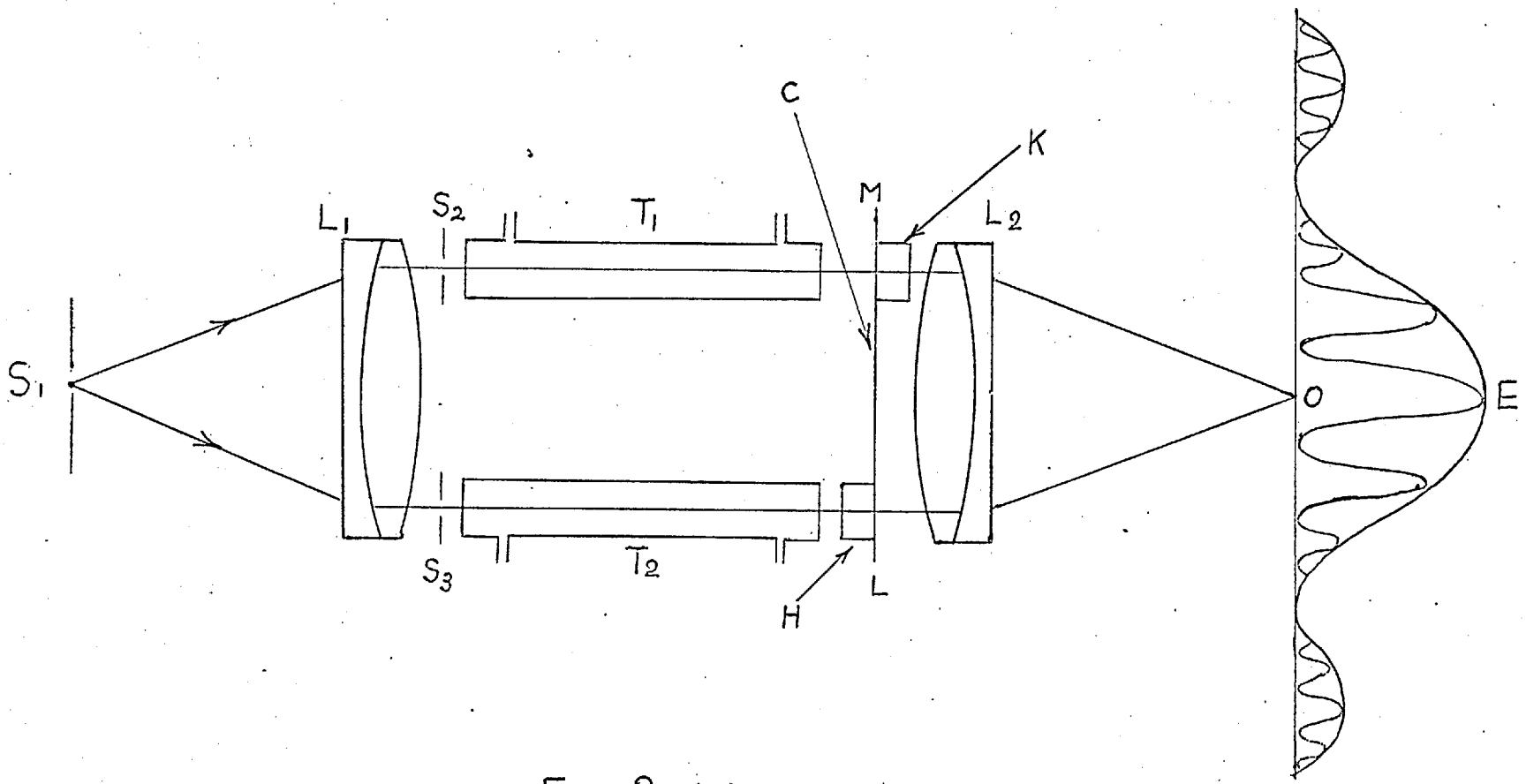

Fig. 2. (a.)

which are viewed with the help of eye piece E. The fringes first observed when the two tubes T_1 and T_2 are empty, and gas is then introduced in the tube T_2, which will produce a difference in optical path length between T_2 and T_1. If the refractive index of the gas let into one of the tubes is $\delta\mu$, a path difference $\delta s = t\delta\mu$ (t being the length of each tube) is introduced, and the fringes are displaced from their former position. The difference of refractive index may be measured by observing fringe shift directly or more conveniently by the compensation method considered below.

As an improvement a compensator, known as the Jamin compensator, is employed. This is shown in Fig. 2(b). It consists of two glass plates H and K fixed to a common axis LM and inclined to one another at a small angle. This arrangement can be rotated as a whole about LM and the rotation is indicated on a circular scale. The compensator is mounted as shown in Fig. 2(a), such that LM is horizontal and one plate lies in the path of each of the beams traversing the tubes T_1, T_2. It will be seen that if the rays pass through the plates at different angles an optical path difference is introduced and this is varied as the compensator is rotated as a whole. By employing monochromatic light and observing the passage of fringes across the field of view as the compensator is rotated, the scale can be calibrated to read optical path differences in terms of wave length. By varying the angle between the compensator plates, the sensitivity of the device is changed, being greater when the inclination between the plates is reduced, since a

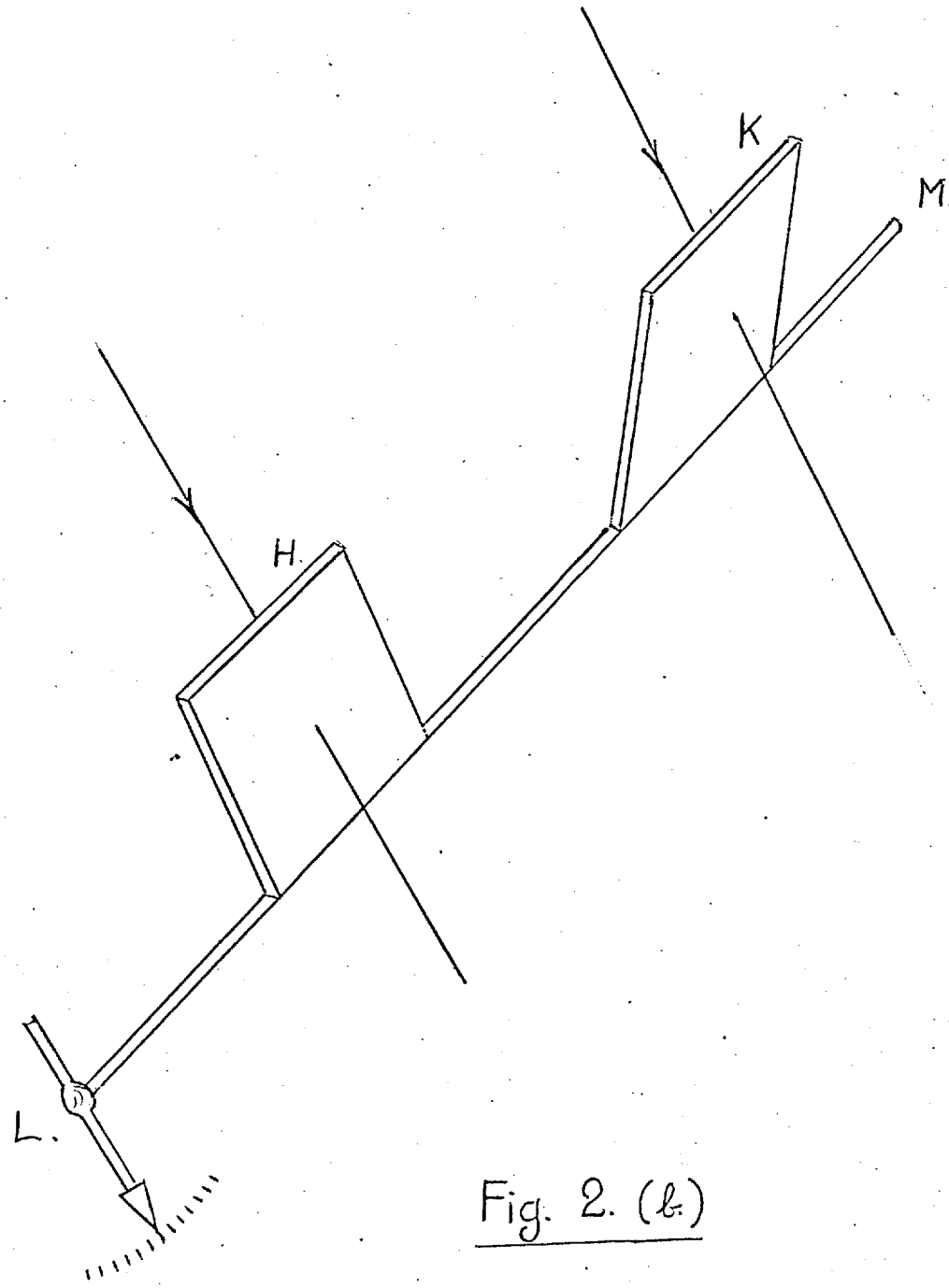

Fig. 2. (b.)

larger rotation is required to introduce a given optical path difference. The setting requires a judgement of the position of fringes relative to a fixed reference, and the precision obtained does not exceed $\frac{\lambda}{40}$ even under good conditions.

In order to have a more sensitive and stable arrangement Zernike proposed a three-slit interferometer, based on Rayleigh's form, where the judgement to be made is one of equal intensity. This method can be more stable, and the estimated sensitivity is also much greater, being $\frac{\lambda}{250}$.

In Zernike's three-slit interferometer light beams from the two outer slits combine to form 2-beam fringes. The third beam, after having suffered the path difference to be measured, is superposed upon these fringes. The result is that the fringes are alternately reinforced and weakened in intensity, provided the third beam is not in exact quadri-phase with the 2-beam fringes. This may be explained by reference to Fig. 3. The two beams I and II produce fringes because their wave-fronts are slightly inclined, the maxima being at the points 0, 1, 2, -1, -2, etc. where the separation of the fronts equals the indicated whole number of wave lengths. If now the wave front III from the central slit bisects the angle between I and II, as shown, the even numbered fringes 0,2 etc. will be reinforced, and the odd numbered ones are weakened by the superposition of III. This is because the phases of alternate fringes in the 2-beam system differ by π. The reverse will occur if beam III has opposite phase. If, however, beam III has a phase

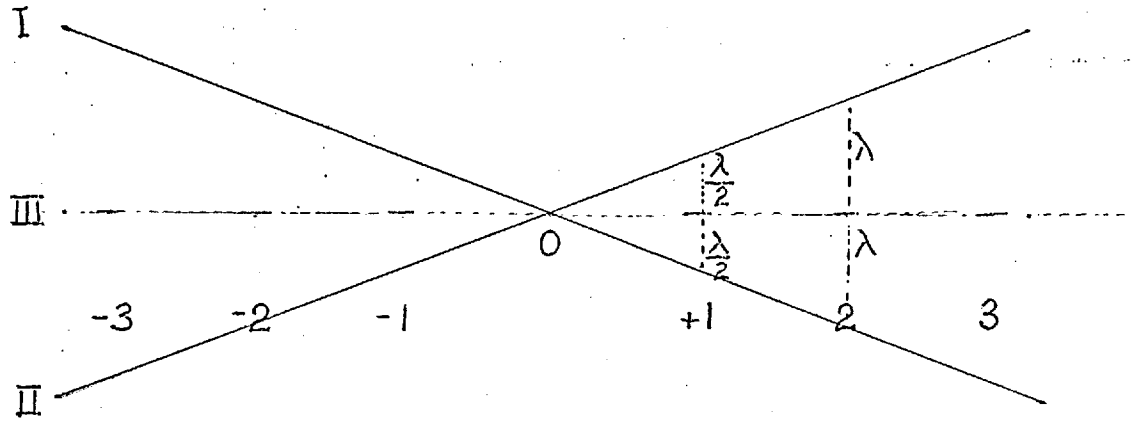

Fig. 3.

difference of $\pm\frac{\pi}{2}$, its intensity will have to be added everywhere, that is to say, that all the fringes will remain of equal intensity. Summarizing this, one can say that fringes of equal intensity are caused by outer slits, together with the coherent background from the middle slit, which alternately reinforces and suppresses these fringes. Zernike proposed the following practical arrangement for this. A screen with three equidistant vertical slits is placed on the table of a large spectrometer and illuminated by parallel light. Beams I and II consist of light which has passed through the outer slits while beam III is one which has passed through the middle one. To equalize the amplitude of beam through the middle slit and those coming from the outer slits, the middle slit can be made twice the width of the outer ones. The fringe system is observed by means of the spectrometer telescope, and the path length compensation is obtained, with no alteration in the intensity of the fringes, by adjusting the position of the eye piece of the telescope along the axis. A phase strip to be measured may be placed behind the middle slit so that it is in the path of the middle or the central beam III. This will result in an outward or inward shift of the eye piece, which can measure the path difference to an accuracy of the order of $\frac{\lambda}{250}$

The experimental arrangement of Zernike's method is shown diagrammatically in Fig. 4. Here parallel light falls on a screen with three slits S_1, S_{11}, S_{111}, when the outer two beams form fringes, with which the middle beam forms the three-beam fringes seen by telescope.

Vittoz proposed another arrangement which is a modification of

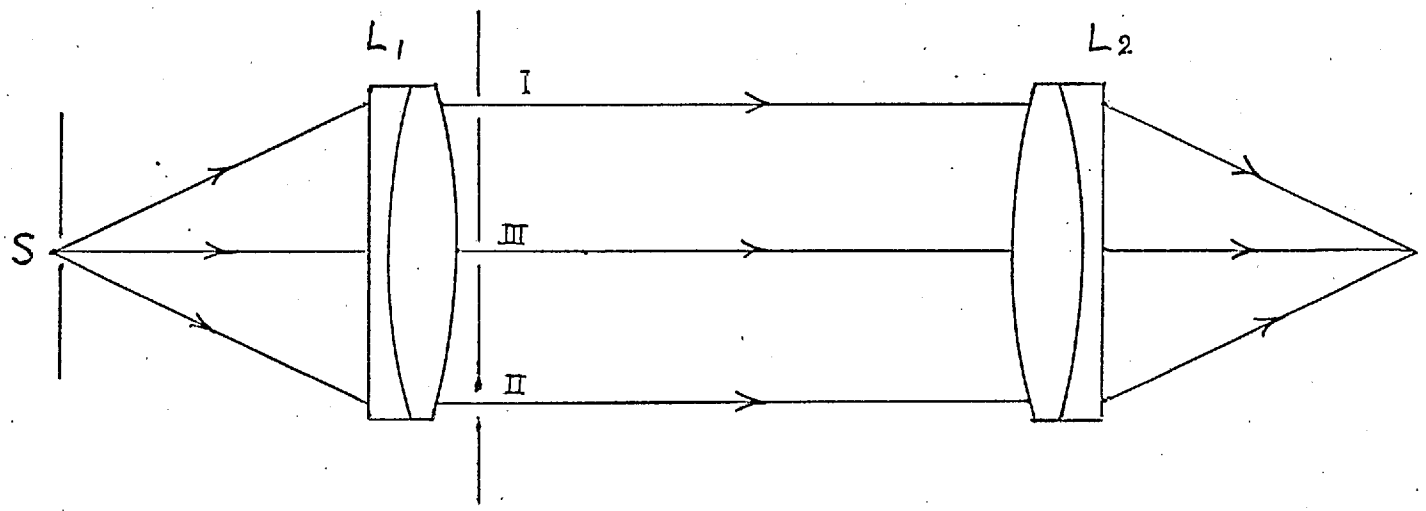

Fig. 4.

Zernike's method. In this he uses a variable phase compensator for the III beam. The arrangement due to Vittoz is shown by Fig. 5.

In Zernike's arrangement, namely the 3-slit analogue of the Rayleigh interferometer, the fringes are formed by the interference of three diffraction patterns, namely the images formed by the three aperture slits of the object slit. The mean intensity and the envelope of the fringes is thus non-uniform. The method of 3-beam interferometry which we propose to study is of Michelson form, which lends itself to photo-detection and higher sensitivity. The lay-out is shown schematically in Fig. 6(a) The source S considered is a pin-hole illuminated by mercury green light. Two-beam fringes are formed by a cube which together with a right angled prism cemented to it forms one arm of the Twyman interferometer. The other arm consists of a pentagonal prism in addition to a right angled prism. This is necessary to avoid reversal of the third beam relative to those forming two-beam fringes, which would result in poor spatial coherence between them.

The plane of best contrast of the 2-beam fringes is at the reflecting faces F of the cube interferometer, and this plane is re-imaged by the lens L to give a real image of the fringes at F'.

The expected form of the fringes, for the case of Fig. 6(b) is shown in Fig. 6(c). While considering Fig. 6(b) it is assumed that we have the ideal conditions, that is the third wavefront is parallel to the line of intersection of the other two and exactly bisects the angle between (1) and (2).

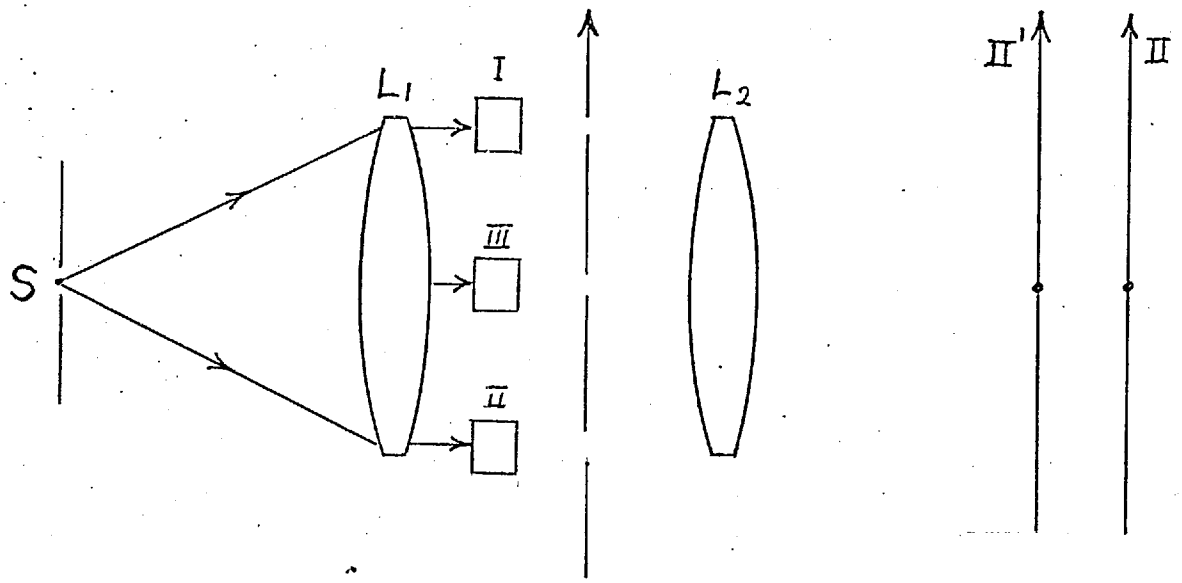

Fig. 5.

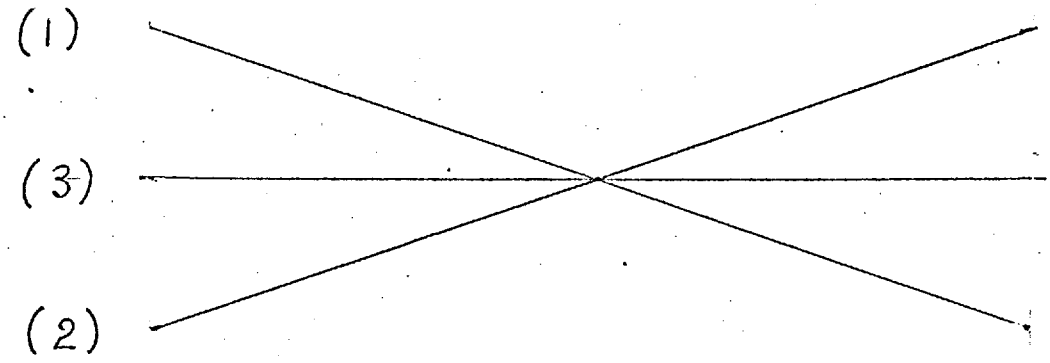

(b)

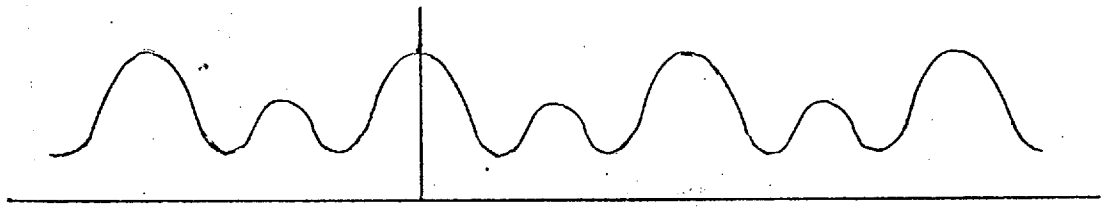

Three beam fringes.

(c)

Fig. 6.

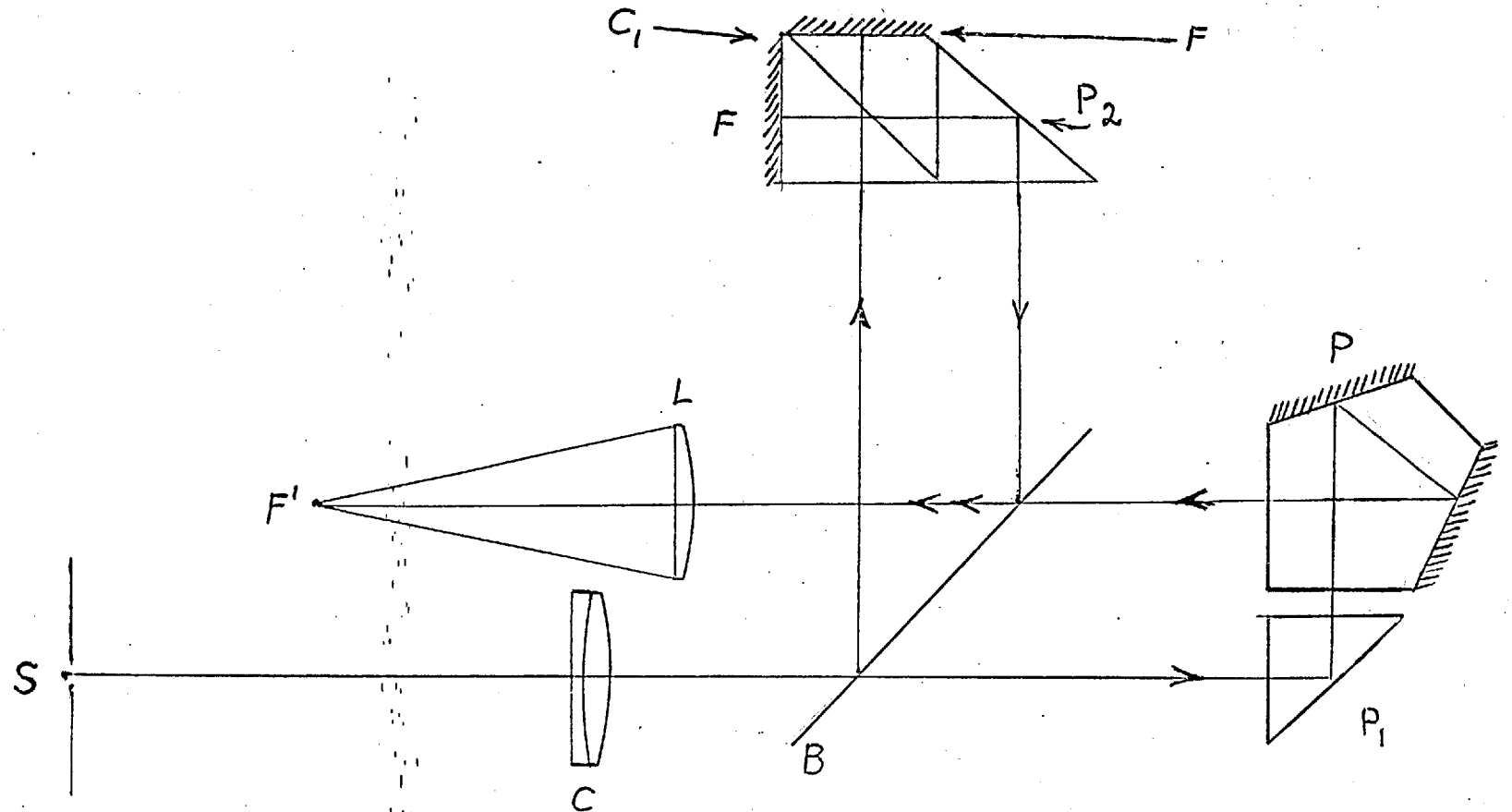

S. Source
C. Collimator
B. Beam-splitter
P. Pentaprism
P_1 Right-angled prism
C_1 Cube Interferometer
P_2 Right-angled prism
L Plano-convex lens.

Fig. 6.

A proposed photo-detection method is as explained below. A scan grating, which is a radial square wave grating, driven at a constant speed by a motor, is placed at the fringe plane F'. Light signals from the grating are fed to a photo-multiplier tube. The out-put of the photo-multiplier is fed to a frequency selective amplifier, and then to a final detecting circuit.

The expected sensitivity of the proposed arrangement for the measurement of path difference is $\frac{\lambda}{700}$

In Fig. 5(b) we have considered ideal conditions. In practice, however, we have various departures present. All these are discussed in detail in the next chapters.

CHAPTER II

Intensity Distribution in the Three-Beam Fringes

In a three beam interferometer three coherent waves contribute to form interference fringes. The interference pattern is conveniently looked upon as the result of interference between the third wave and the coherent fringe pattern resulting from interference of the other two waves.

Ideally, the third wave front should be parallel to the line of intersection of the other two and also parallel to the plane bisecting the other two waves. In practice, however, these conditions will not be fulfilled exactly. Accordingly, an expression will be found for the final intensity distribution obtained when the third wave has both of these components of tilt error. Let the three plane waves be denoted by (1), (2) and (3).

To find the distribution of intensity in the three beam fringes we first find an expression for the complex amplitude produced by the plane waves (1), (2) at a point P in the plane of intersection of the two waves (1) and (2) (see Fig. 1., Fig. 2.). Then the total complex amplitude at P is found when the third plane wave also falls there at a distance d from the line of intersection between (1) and (2), and having both the component of tilt errors mentioned above.

Thus let N_1 and N_2 be the normals to the waves (1) and (2), and let us choose the Y-axis to be perpendicular to the plane

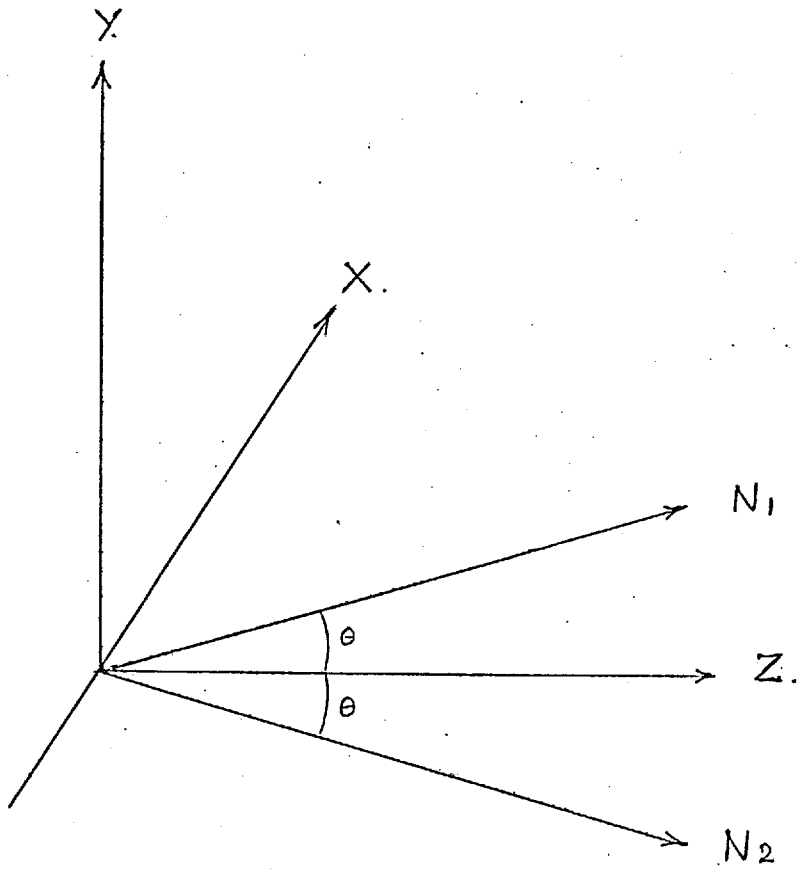

Fig. 1.

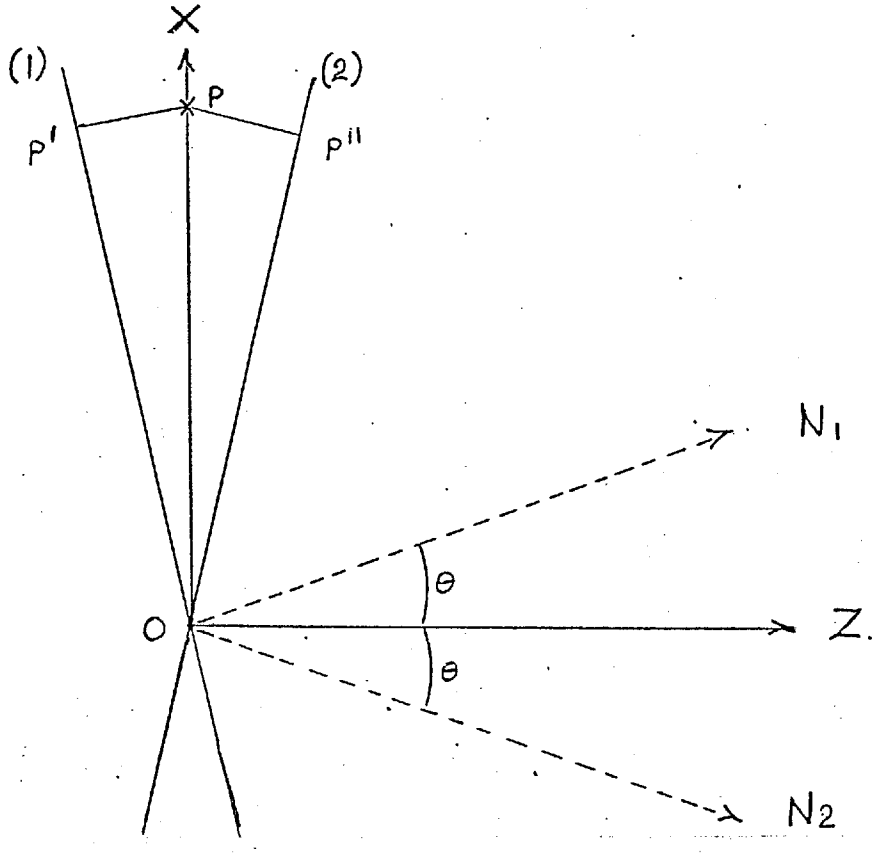

Fig. 2.

(N_1, N_2) and X-and Z-axes such that the Z-axis bisects the angle (N_1, N_2). Let θ be the angle between N_1 and the Z-axis. θ is then also equal to the angle between N_2 and the Z-axis. Suppose now that the two plane waves (1) and (2) fall on the X-Z plane with normals having direction cosines l_1, m_1, n_1 and l_2, m_2, n_2 respectively. Also, let the phases of the two plane waves (1) and (2) be taken to be zero at the point O. The phases of the disturbances produced by (1) and (2) at the point P will be given by $k[P'P]$ and $k[P''P]$ respectively, where $k = \frac{2\pi}{\lambda}$, (fig. 2). The complex amplitudes due to (1) and (2) at the point P will be given by $U_1 = \alpha_1 e^{-ikl_1 x}$ and $U_2 = \alpha_2 e^{-ikl_2 x}$ where α_1 and α_2 are the amplitudes of the waves (1) and (2). Now N_1 has direction cosines $l_1 = \sin\theta$, $m_1 = 0$ and N_2 has direction cosines, $l_2 = -\sin\theta$ and $m_2 = 0$ so that the complex amplitudes of (1) and (2) at P will be given by:

$$U_1 = \alpha_1 e^{-ik \sin\theta x}$$
$$U_2 = \alpha_2 e^{+ik \sin\theta x} \qquad (1)$$

Denote by U_3 the complex amplitude produced at P by the wave (3), which is at a distance d from O, the point of intersection of waves (1) and (2), and whose normal has direction cosines (l, m) relative to the axis OZ (Fig. 3) Then,

$$U_3 = \beta e^{ikd} e^{ik(lx + my)} \qquad (2)$$

where β is the amplitude of the third wave, and $k = \frac{2\pi}{\lambda}$. The zero position of the third wave is shown by the continuous line

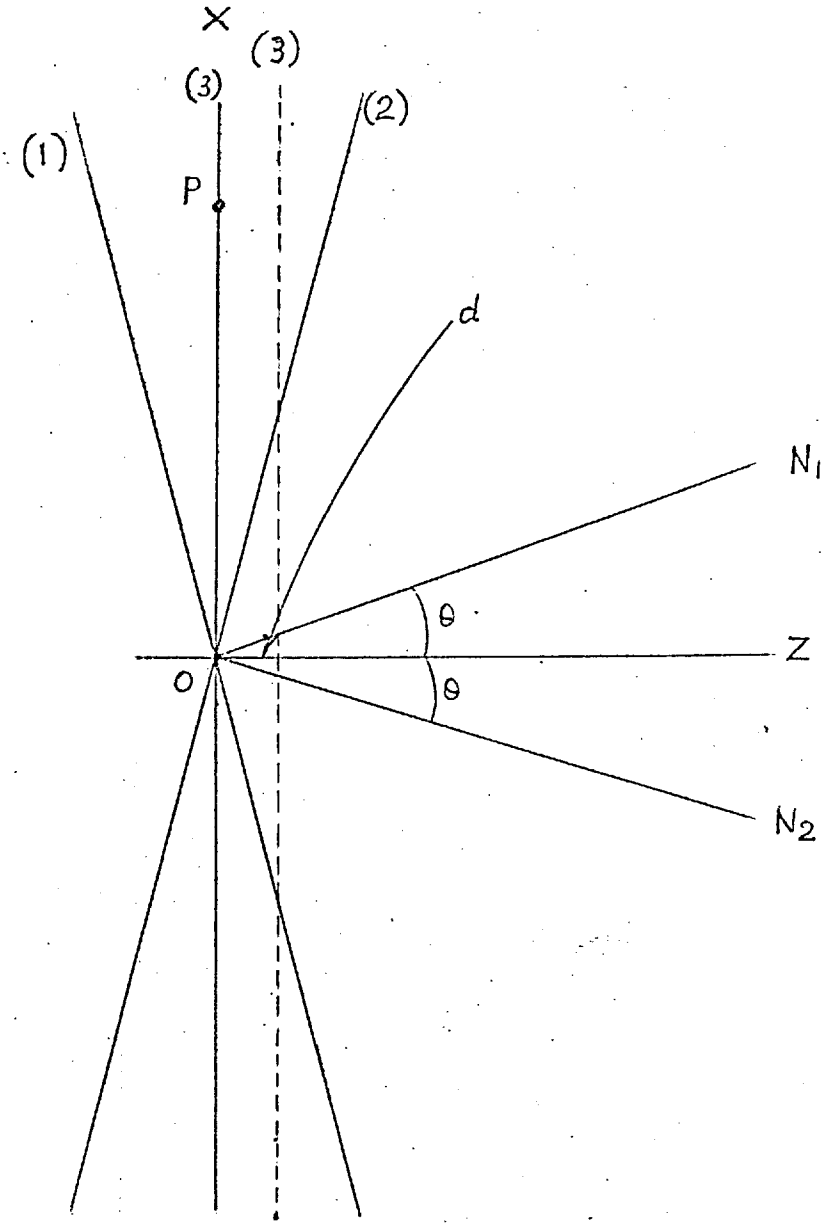

Fig. 3.

while the dotted line shows the third wave when it is phase shifted.

The total complex amplitude at the point P is now given by

$$U = U_1 + U_2 + U_3$$

and the distribution of intensity in the fringes will be given by

$$I_p = |U|^2 = |U_1 + U_2 + U_3|^2$$

that is, by

$$\begin{aligned} I_p = {} & |U_1|^2 + |U_2|^2 + |U_3|^2 \\ & + U_1^* U_2 + U_2^* U_3 + U_1 U_2^* \\ & + U_2 U_3^* + U_3^* U_1 + U_1 U_3^* \end{aligned} \qquad (3)$$

where * denotes the complex conjugate. Substituting for U_1, U_2 and U_3 from (1) and (2) in (3) and rearranging the various terms we get,

$$\begin{aligned} Ip = {} & a_1^2 + a_2^2 + 2a_1 a_2 \cos(2k \sin\theta x) \\ & + \beta^2 + 2\beta(a_2 + a_1)\cos\left[k(lx+my)+kd\right] \cos(k\sin\theta x) \\ & + 2\beta(a_2 - a_1) \sin\left[k(lx+my)+kd\right] \sin(k\sin\theta x) \end{aligned} \qquad (4)$$

It is now convenient to make the substitution $d = (\epsilon - \frac{1}{4})\lambda$ and (4) then becomes

$$\begin{aligned} Ip = {} & a_1^2 + a_2^2 + 2a_1 a_2 \cos(2k\sin\theta x) \\ & + \beta^2 + 2\beta(a_2 + a_1) \sin\left[k(lx + my) + 2\pi\epsilon\right] \cos(k\sin\theta x) \\ & + 2\beta(a_2 - a_1)\cos\left[k(lx + my) + 2\pi\epsilon\right] \sin(k\sin\theta x) \end{aligned} \qquad (5)$$

Expression (5) gives the distribution of intensity in the three beam fringes when the beams (1) and (2) are assumed to have unequal amplitudes, namely a_1 and a_2 respectively, and beam three has tilt errors.

If we consider a tilt free system, that is $l = m = o$, (5) becomes,

$$Ip = I_o + \beta^2 + 2\beta(a_2 + a_1)\text{Sin } 2\pi e \text{ Cos}(k\text{Sin}\Theta x) + 2\beta(a_2 - a_1)\text{Cos } 2\pi e \text{ Sin}(k \text{ Sin}\Theta x) \quad (6)$$

where $I_o = a_1^2 + a_2^2 + 2a_1a_2 \text{ Cos}(2k \text{ Sin}\Theta x)$

is the intensity distribution which would be given by the two-beam fringes alone.

To explain this further, the curves corresponding to different terms in (6) are shown in Fig. 4. There, (a) represents the intensity distribution, I_o, in the two beam fringes; (b) shows that due to the constant term β^2 plus the cosine; and (c) shows the sine term. The curve of Ip is the sum of those in (a), (b) and (c). Clearly, the effect of (a) plus (b) will be to produce fringes on a background intensity, in which the fringes $0, \pm 2, \pm 4, \ldots$, are increased in intensity, while the fringes $\pm 1, \pm 3, \ldots$, are reduced in intensity. Thus, in the absence of (c), the even fringes will have maxima of intensity,

$$Ip = a_1^2 + a_2^2 + 2a_1a_2 + \beta^2 + 2\beta(a_1 + a_2)\text{Sim } 2\pi e = (a_1 + a_2)^2 + \beta^2 + 2(a_1 + a_2)\beta \text{ Sin}(2\pi e) \quad (7)$$

while the odd fringes will have maxima of intensity,

$$Ip = (a_1 + a_2)^2 + \beta^2 - 2(a_1 + a_2)\beta.\text{Sin}(2\pi e) \quad (8)$$

The mean of these maxima is

$$Ip = (a_1 + a_2)^2 + \beta^2 \quad (9)$$

and the difference in intensity between each of the alternate

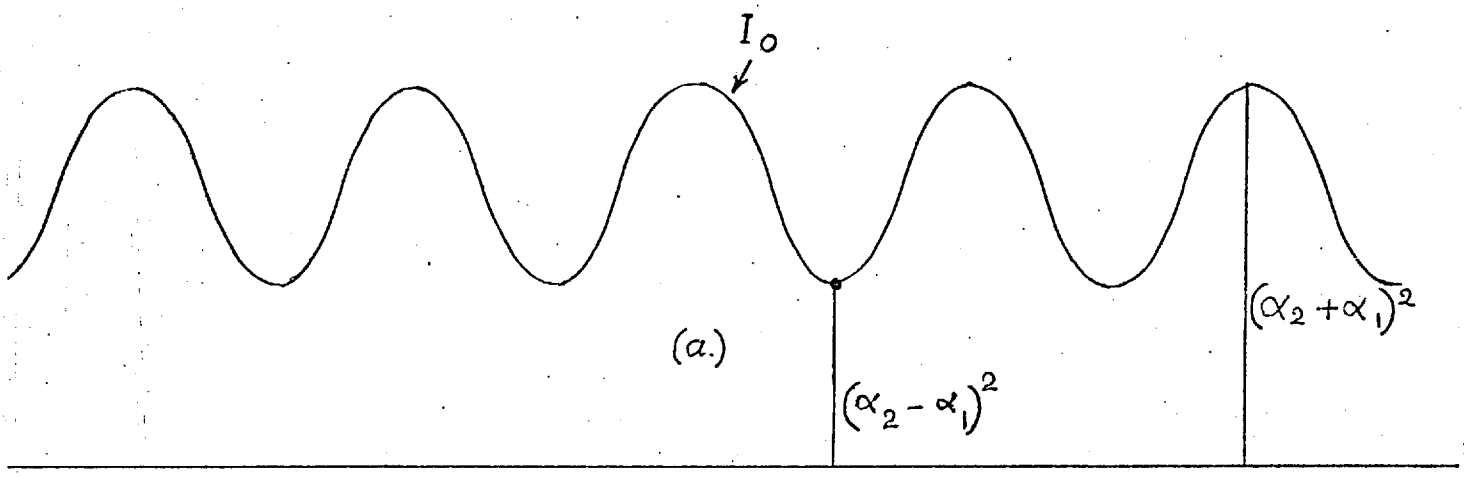
I_o
(a.)
$(\alpha_2 - \alpha_1)^2$
$(\alpha_2 + \alpha_1)^2$

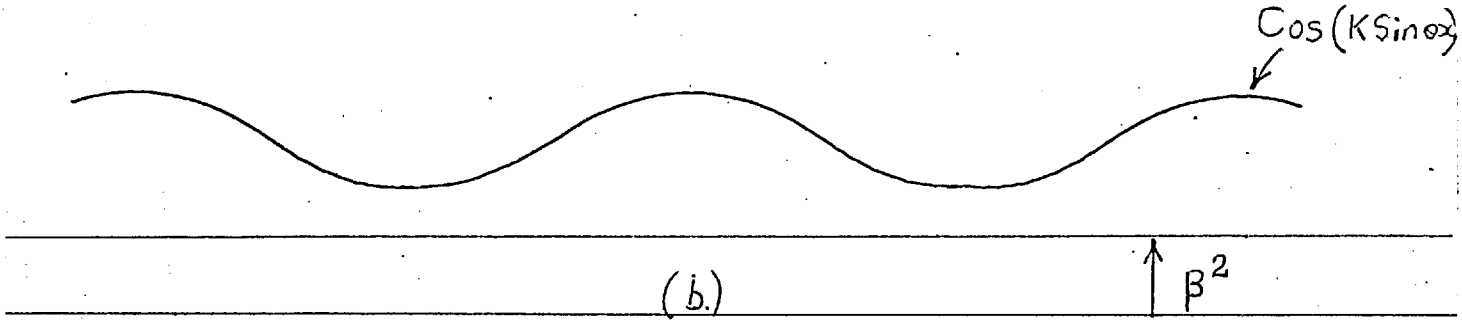
Cos (K Sin θx)
(b.)
β^2

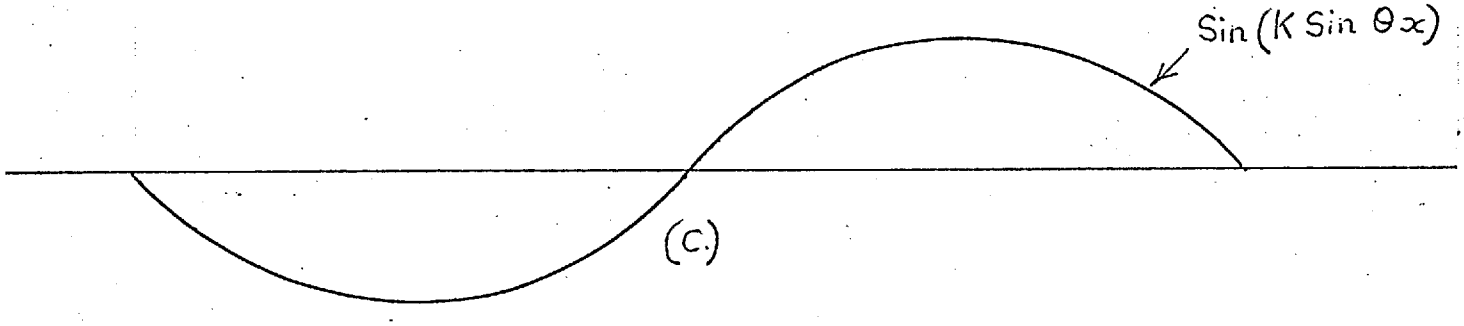
Sin (K Sin θx)
(c.)

Fig. 4.

maxima as a fraction of their mean intensity is

$$\frac{\delta Ip}{Ip} = \frac{4(\alpha_1 + \alpha_2)\beta}{(\alpha_1 + \alpha_2)^2 + \beta^2} \quad \text{Sin } (2\pi\epsilon) \qquad (10)$$

Now, c is only absent when $\alpha_1 = \alpha_2$, or writing α for each of these,

$$\frac{\delta Ip}{Ip} = \frac{8\alpha\beta}{4\alpha^2 + \beta^2} \quad \text{Sin } (2\pi\epsilon) \qquad (11)$$

To obtain an estimate of the expected sensitivity, put $\alpha = \sqrt{2}\ \beta$ and $\text{Sin}(2\pi\epsilon) = 2\pi\epsilon$, and assume that the minimum detectable δIp is 2% of Ip so that $\frac{\delta Ip}{Ip} = 0{\cdot}02$. Then,

$$\epsilon = \frac{\delta p}{\lambda} \approx \frac{0{\cdot}02}{3{\cdot}8\pi} \qquad (12)$$

where δ p is the difference in path length, the above formula gives

$$\delta p \approx \frac{\lambda}{600} \qquad (13)$$

and this represents an order of magnitude improvement in sensitivity over conventional fringe setting methods.

It will be noted, however, that unequal amplitudes for waves (1) and (2) will introduce asymmetry into the fringe pattern, and impair the accuracy. The amplitude of the term (c) is $2\beta(\alpha_2-\alpha_1)$ Cos $(2\pi\epsilon)$, and is thus equal to $2\beta(\alpha_2-\alpha_1)$ when $\epsilon \approx o$, which is at the desired setting. The two beams (1) and (2) thus need to be of equal amplitude to a high degree of precision. This is assured more easily in the arrangement proposed here, as is shown in Fig. 5(a) of Chapter I. It requires only that the reflecting faces of the Michelson cube interferometer be equal, and this is not difficult to achieve. On the other hand, to arrange that the outer slits in the Rayleigh form

of interferometer be equal in width to, say, $\pm$ 1% is not easy. It would seem, moreover, that previous workers havenot appreciated this important factor in 3-beam interferometry. Again, as mentioned earlier, the fringe pattern is not uniform in the case of the Rayleigh interferometer, whereas with the Michelson variant uniform 3-beam fringes are obtained. This is useful if a photo-electric scanning technique is to be used to determine the null setting.

It was for these reasons that the present study was under-taken, together with the advantage of the Michelson over the Rayleigh form in the matter of the maximum source size giving good fringe contrast. This advantage is also preserved in the 3-beam forms, in that the three rays intersecting at any point in the fringe plane can be made to derive from almost exactly the same ray leaving the source.

A more detailed theoretical treatment, and an account of the fringe scanning technique will be given in what follows below.

2) Photo-electric Detection

Nearly all the detection systems are operated with an alternating signal at some convenient frequency. This is done partly because it is convenient to amplify alternating current, as compared with the direct current, and also because detection systems operating on a direct current basis are subject to drifts and changes in sensitivity to which a.c. systems are not. Thus

direct fringe scanning methods have the serious drawback that any fluctuations in light intensity can lead to errors. Also, since noise represents the ultimate limit on the sensitivity of a detecting system, we requirea method in which this is reduced to a minimum.

It is here proposed to use a scan grating which is a square wave radial grating moving with constant speed. If the grating has a period Po and is moving with a uniform speed, as it moves across the series of sine waves of intensity, a detector placed to accept the total light transmitted will only produce a constant signal provided the sine wave components present have periods equal to Po, $\frac{Po}{2}$ ..... $\frac{Po}{3}$ .... $\frac{Po}{n}$. These are the spatial frequencies corresponding to the fundamental and harmonics of the grating. The form of the electrical output from a photo-electric detector of this total light is a periodic signal.

The intensity distribution in the fringes, given by (4) is of the form

$$\begin{aligned} Ip = {} & (2\alpha^2+\beta^2)+\alpha^2\left[e^{2ik\mathrm{Sin}\theta x} + e^{-2ik\mathrm{Sin}\theta x}\right] \\ & +\alpha\beta e^{ikd}\left[e^{ik(\mathrm{Sin}\theta+\ell)x} + e^{-ik(\mathrm{Sin}\theta-\ell)x}\right] \\ & e^{ikmy} + \alpha\beta e^{-ikd}\left[e^{ik(\mathrm{Sin}\theta-\ell)x} + e^{-ik(\mathrm{Sin}\theta+\ell)x}\right] \\ & e^{-ikmy} \end{aligned} \qquad (14)$$

where it is now assumed that $a_1 = a_2 = \alpha$. The scan grating is placed at the real image of the fringes. Let the transparency at the point x of the grating at time $t = o$ be denoted by $Z(X)$ Since $Z(X)$ is periodic, of period Po, write,

$$Z(X) = \sum_{n=-\infty}^{+\infty} Zn\ e^{-i\frac{2\pi n}{Po}x} \qquad (15)$$

in terms of which the transparency at time t is given by

$$Z(X - \gamma t) = \sum_{n=-\infty}^{+\infty} Zne^{-i\frac{2\pi n}{Po}(X - \gamma t)} \qquad (16)$$

that is,

$$Z(X - \gamma t) = \sum_{n=-\infty}^{+\infty} Zne^{-i\frac{2\pi n}{Po}X}\ e^{+i\frac{2\pi n}{Po}\gamma t} \qquad (17)$$

where γ is the peripheral velocity with which the scan grating is moving. It is convenient to use the spatial frequency in place of Po. Thus, let $\sigma_o = \frac{1}{Po}$ be the spatial frequency of the grating. Also let $\frac{\gamma}{Po} = \nu$ and $n\nu = fn$ be used to denote the temporal frequencies. Then (17) can be written

$$Z(x-\gamma t) = \sum_{n=-\infty}^{+\infty} Zne^{-i2\pi n\sigma_o x}\ e^{i2\pi n f_n t} \qquad (18)$$

Now the total light flux transmitted by the grating when illuminated with the fringes is

$$F(t) = \int_{-Xo}^{+Xo}\int_{-Yo}^{+Yo} Ip\ Z(x-\gamma t)\,dx\,dy \qquad (19)$$

or substituting for $Z(X - \gamma t)$ from (18)

$$F(t) = \sum_{n=-\infty}^{+\infty} Zn\left\{\int_{-Xo}^{+Xo}\int_{-Yo}^{+Yo} Ip\,e^{-i2\pi n\sigma_o x}\,dx\,dy\right\}e^{i2\pi fnt}$$

The fringes are here assumed to be limited by a rectangular aperture of height 2Yo and width 2Xo. This is a periodic function of time, with fundamental frequency $f_1 = \nu = \frac{\gamma}{Po} = \gamma\sigma_o$ The expression (19a) gives the total light flux seen looking through the grating. It contains a D.C. term and an A.C. term. The D.C. term is of amplitude

$$Fo = Zo \int_{-Xo}^{Xo}\int_{-Yo}^{Yo} Ip.\,dx\,dy \qquad (20)$$

and the complex amplitude of the fundamental A.C. term is

$$F_1 = 2Z_1 \int_{-Xo}^{+Xo}\int_{-Yo}^{+Yo} Ip\,e^{i2\pi\sigma_o x}\,dx\,dy \qquad (21)$$

The values of these amplitudes may thus be found by substituting the appropriate form for Ip in the integrals. It may be seen that F_o and F_1 are simply the values of the 2-dimensional Fourier transform of Ip = I (x y) for the spatial frequency pair (o, σ_o) and (o, σ_o) respectively. In order to find the value of F_o, substitute for Ip from (14) in (20), giving

$$F_o = Z_o \left\{ \int_{-X_o}^{+X_o} \int_{+Y_o}^{+Y_o} \left\{ (2\alpha^2+\beta^2)+\alpha^2 \left[e^{2ik\sin\theta.x} + e^{-2ik\sin\theta.x} \right] \right.\right.$$

$$+\alpha\beta\ e^{ikd} \left[e^{ik(\sin\theta+1)x} + e^{-ik(\sin\theta-1)x} \right]$$

$$\left.\left. .e^{ikmy} + \alpha\beta e^{-ikd} \left[e^{ik(\sin\theta-1)x} + e^{-ik(\sin\theta+1)x} \right] e^{-ikmy} \right\} \ dxdy \right\} \qquad (22)$$

$$F_o = Z_o \left\{ \int_{-X_o}^{+X_o} \int_{+Y_o}^{+Y_o} (2\alpha^2+\beta^2)dxdy + \alpha^2 \int_{-X_o}^{+X_o} \int_{-Y_o}^{+Y_o} \left[e^{2ik\sin\theta.x} \right.\right.$$

$$\left. + e^{-2ik\sin\theta.x} \right] dxdy + \alpha\beta \int_{-X_o}^{+X_o} \int_{-Y_o}^{+Y_o} e^{ikd} \left[e^{ik(\sin\theta+1)x} + e^{-ik(\sin\theta-1)x} \right] e^{ikmy} dxdy$$

$$\left. + \alpha\beta \int_{-X_o}^{+X_o} \int_{-Y_o}^{+Y_o} e^{-ikd} \left[e^{ik(\sin\theta-1)x} + e^{-ik(\sin\theta+1)x} \right] e^{-ikmy} dxdy \right\} \qquad (23)$$

The various integrals when evaluated give the following:

$$\int_{-X_o}^{+X_o} \int_{-Y_o}^{+Y_o} (2\alpha^2+\beta^2)\ dxdy = 4x_o Y_o (2\alpha^2+\beta^2)$$

$$\alpha^2 \int_{-X_o}^{+X_o} \int_{+Y_o}^{+Y_o} (e^{2ik\sin\theta.x} - e^{-2ik\sin\theta.x})\ dxdy = \frac{2Y_o\alpha^2\ 4\sin(2k\sin\theta.x_o)}{2k\sin\theta.}$$

$$\alpha\beta \int_{-X_o}^{+X_o} \int_{-Y_o}^{+Y_o} e^{ikd} \left[e^{ik(\sin\theta+1)x} + e^{-ik(\sin\theta-1)x} \right] e^{ikmy}\ dxdy$$

$$= \alpha\beta \frac{2Y_o \text{ Sin } kmY_o}{kmY_o} \left[e^{ikd} \left\{ \frac{\text{Sin } \left[k(\text{Sin } \theta+1\right] x_o}{\left[k(\text{Sin } \theta+1)\right]} + \frac{2 \text{ Sin} \left[k(\text{Sin } \theta-1)X_o\right]}{\left[k(\text{Sin } \theta-1)\right]} \right\} \right]$$

$$\alpha\beta \int_{-X_o}^{+X_o} \int_{-Y_o}^{+Y_o} \bar{e}^{ikd} \left[e^{ik(\text{Sin } \theta-1)X} + \bar{e}^{ik(\text{Sin } \theta+1)X} \right] e^{ikmy} dxdy$$

$$= \alpha\beta \frac{2Y_o \text{ Sin } kmY_o}{kmY_o} \left[\bar{e}^{ikd} \left\{ \frac{2\text{Sin}\left[k(\text{Sin } \theta-1)X_o\right]}{\left[k(\text{Sin } \theta-1)\right]} + \frac{2\text{Sin}\left[k(\text{Sin } \theta+1)X_o\right]}{\left[k(\text{Sin } \theta+1\right]} \right\} \right]$$

Substituting these integrals in (23) and rearranging the terms we get,

$$F_o = 4X_oY_oZ_o \left\{ (2\alpha^2 + \beta^2) + 2\alpha^2 \frac{\text{Sin}(2k \text{ Sin } \theta. X_o)}{(2 \text{ k Sin } \theta. X_o)} + 2\alpha\beta \frac{\text{Sin } kmY_o}{kmY_o} \right.$$

$$\left. \left[\frac{\text{Sin}\left[k(\text{Sin } \theta+1)X_o\right]}{\left[k(\text{Sin } \theta+1)X_o\right]} + \frac{\text{Sin}\left[k(\text{Sin } \theta-1)X_o\right]}{\left[k(\text{Sin } \theta-1)X_o\right]} \right] \text{Cos } kd \right\} \qquad (24)$$

which gives the amplitude of the D.C. component.

Again, from (21 we have

$$F_1 = 2Z_1 \int_{-X_o}^{+X_o} \int_{-Y_o}^{+Y_o} \text{Ip } \bar{e}^{i2\pi\sigma_o X} \, dxdy \qquad (25)$$

and substituting for Ip from equation (14) we get

$$F_1 = 2Z_1 \int_{-X_o}^{+X_o} \int_{-Y_o}^{+Y_o} (2\alpha^2+\beta^2) \, \bar{e}^{i2\pi\sigma_o X} \, dxdy + \alpha^2 \int_{-X_o}^{+X_o} \int_{-Y_o}^{+Y_o} \left[e^{2ik\text{Sin } \theta. X} \right.$$

$$\left. + \bar{e}^{2ik\text{Sin } \theta. X} \right] dxdy + \alpha\beta \int_{-X_o}^{+X_o} \int_{-Y_o}^{+Y_o} e^{ikd} \left[e^{ik(\text{Sin } \theta+1)X} - \bar{e}^{ik(\text{Sin } \theta-1)X} \right].$$

$$\bar{e}^{ikmy} \, dxdy + \alpha\beta \int_{-X_o}^{+X_o} \int_{-Y_o}^{-Y_o} \bar{e}^{ikd} \left[e^{ik(\text{Sin } \theta-1)X} \, \bar{e}^{ik(\text{Sin } \theta+1)X} \right] e^{ikmy} \, dxdy \qquad (26)$$

The following notations will now be used

$$p \sin\theta = \frac{\lambda}{2}$$

$$\sigma = \frac{1}{p} = \frac{2\sin\theta}{\lambda}$$

$$k \sin\theta = \frac{2\pi \sin\theta}{\lambda} = \pi\sigma \qquad (27)$$

$$u = {}^{l}/_{\lambda}$$

$$v = {}^{m}/_{\lambda}$$

where p is the spacing of the 2-beam fringes, λ the wavelength of the light and θ the half-angle between waves (1) and (2). Thus σ is the spatial frequency of the 2-beam fringes. Also, since (l, m) are the direction cosines of the normal to the wave (3), (u, v) are reduced direction cosines giving the components of tilt error. With the above substitutions (27), the expression (26) becomes

$$F_1 = 2Z_1 \left\{ \int_{-X_o}^{+X_o} \int_{-Y_o}^{+Y_o} (2\alpha^2+\beta^2) e^{-i2\pi\sigma_o x}\, dxdy + \alpha^2 \int_{-X_o}^{+X_o} \int_{-Y_o}^{+Y_o} \left[e^{i2\pi\sigma x} + e^{-i2\pi\sigma x} \right] e^{-i2\pi\sigma_o x}\, dxdy \right.$$

$$+\alpha\beta e^{ikd} \int_{-X_o}^{+X_o} \int_{-Y_o}^{+Y_o} \left[e^{i2\pi(\frac{\sigma}{2}+u)} + e^{-i(\frac{\sigma}{2}-u)2\pi} \right] e^{i2\pi vy} e^{-i2\pi\sigma_o x}\, dxdy$$

$$\left. +\alpha\beta e^{-ikd} \int_{-X_o}^{+X_o} \int_{-Y_o}^{+Y_o} \left[e^{i2\pi(\frac{\sigma}{2}-u)} + e^{-i2\pi(\frac{\sigma}{2}+u)} \right] e^{-i(2\pi vy)} e^{-i(2\pi\sigma_o x)}\, dxdy \right\} \qquad (28)$$

The various integrals in the above expression give the following:

$$\int_{-X_o}^{+X_o} \int_{-Y_o}^{+Y_o} \left[2\alpha^2+\beta^2 \right] e^{-i2\pi\sigma_o x}\, dxdy = (2\alpha^2+\beta^2) 2y_o \cdot \frac{\sin(2\pi\sigma_o x_o)}{\pi\sigma_o}$$

$$\alpha^2 \int_{-X_o}^{+X_o} \int_{-Y_o}^{+Y_o} \left[e^{i2\pi\sigma x} + e^{-i2\pi\sigma x} \right] e^{-i2\pi\sigma_o x}\, dxdy$$

$$= 2y_o\, \alpha^2 \left[\frac{\sin 2\pi(\sigma-\sigma_o)x_o}{\pi(\sigma-\sigma_o)} + \frac{\sin 2\pi(\sigma+\sigma_o)x_o}{\pi(\sigma+\sigma_o)} \right]$$

$$\alpha\beta \int_{-X_o}^{+X_o}\int_{-Y_o}^{+Y_o} e^{ikd}\left[e^{i2\pi(\frac{\sigma}{2}+u)}+e^{-i2\pi(\frac{\sigma}{2}-u)}\right] e^{i2\pi vy}\, e^{-i2\pi\sigma_o x}\, dxdy$$

$$=2Y_o\, e^{ikd}\,\frac{\mathrm{Sin}(2\pi vY_o)}{(2\pi vY_o)}\left[\frac{\mathrm{Sin}\,2\pi(\frac{\sigma}{2}+u-\sigma_o)x_o}{\pi(\frac{\sigma}{2}-u+\sigma_o)}+\frac{\mathrm{Sin}2\pi(\frac{\sigma}{2}-u+\sigma_o)x_o}{\pi(\frac{\sigma}{2}-u+\sigma_o)}\right]$$

$$\alpha\beta \int_{-X_o}^{+X_o}\int_{-Y_o}^{+Y_o} e^{-ikd}\left[e^{i2\pi(\frac{\sigma}{2}-u)x}+e^{-i2\pi(\frac{\sigma}{2}+u)x}\right] e^{-i2\pi vy}.e^{-i2\pi\sigma_o x}\, dxdy$$

$$=2y_o\,\frac{\mathrm{Sin}(2\pi vY_o)}{(2\pi vY_o)}\,\alpha\beta\cdot e^{-ikd}\left[\frac{\mathrm{Sin}2\pi(\frac{\sigma}{2}-u-\sigma_o)x_o}{\pi(\frac{\sigma}{2}-u-\sigma_o)}+\frac{\mathrm{Sin}2\pi(\frac{\sigma}{2}+u+\sigma_o)x_o}{\pi(\frac{\sigma}{2}+u+\sigma_o)}\right]$$

and the expression (28) can thus be written

$$F_1=2Z_1\,4x_oY_o\left\{(2\alpha^2+\beta^2)\,\frac{\mathrm{Sin}(2\pi\sigma_o x_o)}{(2\pi\sigma_o x_o)}+\alpha^2\left[\frac{\mathrm{Sin}\,2\pi(\sigma-\sigma_o)x_o}{2\pi(\sigma-\sigma_o)x_o}+\frac{\mathrm{Sin}2\pi(\sigma+\sigma_o)x_o}{2\pi(\sigma+\sigma_o)x_o}\right]\right.$$

$$+\alpha\beta\frac{\mathrm{Sin}(2\pi vY_o)}{(2\pi vY_o)}\left[\frac{\mathrm{Sin}\left[2\pi(\frac{\sigma}{2}+u-\sigma_o)x_o\right]}{\left[2\pi(\frac{\sigma}{2}+u-\sigma_o)x_o\right]}+\frac{\mathrm{Sin}\left[2\pi(\frac{\sigma}{2}-u+\sigma_o)x_o\right]}{\left[2\pi(\frac{\sigma}{2}-u+\sigma_o)x_o\right]}\,e^{ikd}\right.$$

$$\left.\left.+e^{-ikd}\left(\frac{\mathrm{Sin}\left[2\pi(\frac{\sigma}{2}-u-\sigma_o)x_o\right]}{\left[2\pi x_o(\frac{\sigma}{2}-u-\sigma_o)\right]}+\frac{\mathrm{Sin}\left[2\pi(\frac{\sigma}{2}+u+\sigma_o)x_o\right]}{\left[2\pi(\frac{\sigma}{2}+u+\sigma_o)x_o\right]}\right)\right]\right\} \qquad (29)$$

giving the amplitude of the fundamental in the A.C. components of the total light flux F(t).

For a perfectly adjusted system with no tilt between the wave (3) and the bisecting plane of (1) and (2), as illustrated

above in Fig. 5., the parameters have the values $\sigma = 2\sigma_0$; $u = v = 0$ The first of these conditions assumes that the spatial frequency of the fringes matches exactly that of the grating. For such a perfectly adjusted system the expression for Fo, namely (24) becomes,

$$F_o = 4 Z_o X_o Y_o \left\{ (2\alpha^2 + \beta^2) + 2\alpha^2 \frac{\sin(4\pi\sigma_0 X_o)}{(4\pi\sigma_0 X_o)} + 4\alpha\beta \frac{\sin(2\pi\sigma_0 X_o)}{(2\pi\sigma_0 X_o)} \cos kd \right\} \qquad (30)$$

and from (29) F_1 is given by

$$F_1 = 8 Z_1 X_o Y_o \left\{ (2\alpha^2 + \beta^2) \frac{\sin(2\pi\sigma_0 X_o)}{(2\pi\sigma_0 X_o)} + \alpha^2 \left[\frac{\sin(2\pi\sigma_0 X_o)}{(2\pi\sigma_0 X_o)} + \frac{\sin[2\pi(3\sigma_0)X_o]}{[2\pi(3\sigma_0)X_o} \right] + 2\alpha\beta \left(1 + \frac{\sin[2\pi(2\sigma_0)X_o]}{[2\pi(2\sigma_0)X_o]} \right) \cos kd \right\} \qquad (31)$$

Further, let there be an exactly even number of fringes, N, in the length of the grating, 2Xo. With the notation (27) , N is given by $2\sigma X_o = N$, that is $\sigma X_o = \frac{N}{2}$ Also, let N_o be integral and represent the number of grating periods. Then $2\sigma_0 X_o = N_o$, σ_0 being the fundamental spatial frequency of the grating. In the present case $N = 2N_o$, and so, from (30) we get,

$$F_o = 4 Z_o X_o Y_o \left\{ (2\alpha^2 + \beta^2) + 2\alpha^2 \frac{\sin(2N_o\pi)}{(2N_o\pi)} + 4\alpha\beta \frac{\sin(N_o\pi)}{(N_o\pi)} \cos kd \right\}$$

or, N_o being integral,

$$F_o = 4 Z_o X_o Y_o (2\alpha^2 + \beta^2) \qquad (32)$$

Again, from (31) we get, for this case

$$F_1 = 8 Z_1 X_o Y_o \left\{ (2\alpha^2 + \beta^2) \frac{\sin(N_o\pi)}{(N_o\pi)} + \alpha^2 \left[\frac{\sin(N_o\pi)}{(N_o\pi)} + \frac{\sin(3N_o\pi)}{(3N_o\pi)} \right] + 2\alpha\beta \left(1 + \frac{\sin(2N_o\pi)}{(2N_o\pi)} \right) \cos kd \right\}$$

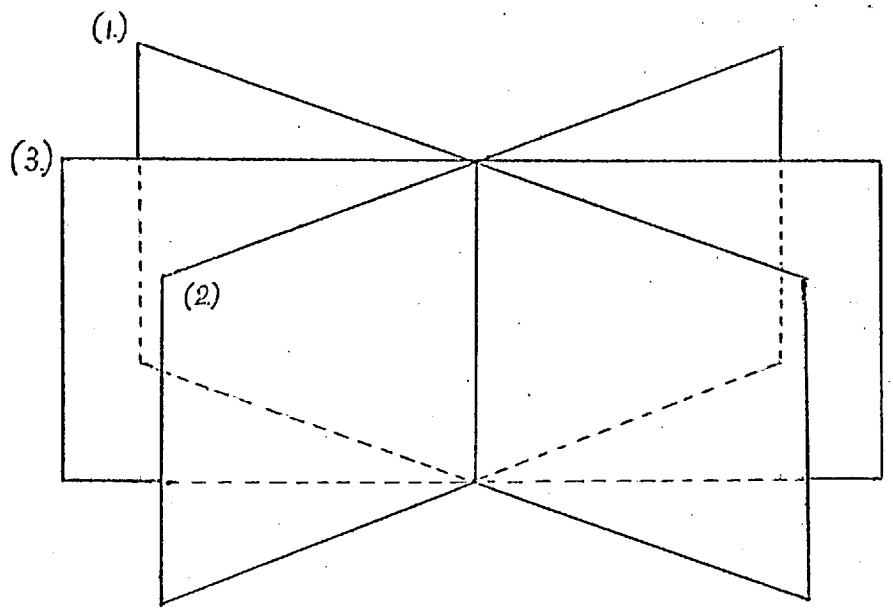

Fig. 5.

or, since No is integral,

$$F_1 = 16\, Z_1\, X_o\, Y_o\, \alpha\beta \cos kd \qquad (33)$$

Again making the substitution

$$d = (\epsilon - \tfrac{1}{4})\lambda$$

the parameter ϵ gives the departure of d from the null-setting value $\pm \frac{\lambda}{4}$. Then F_1 becomes,

$$F_1 = 16\, Z_1\, X_o\, Y_o\, \alpha\beta \sin 2\pi\epsilon \qquad (34)$$

and this gives the amplitude of the A.C. signal which is detected

The sensitivity of the method will be dependent on the signal to noise ratio. The noise will be due predominently to fluctuations in the intensity F_o, and the r.m.s. value of this noise at any frequency will be proportional to $\sqrt{F_o}$, since the fluctuations will be of Poisson type. Thus, the signal to noise ratio will be proportional to

$$\frac{F_1}{\sqrt{F_o}} = \frac{16\, Z_1\, X_o\, Y_o\, 2\beta \sin(2\pi\epsilon)}{\sqrt{4\, Z_o\, X_o\, Y_o\, (2\alpha^2 + \beta^2)}}$$

or

$$\frac{F_1}{\sqrt{F_o}} = 2\left(\frac{Z_1}{\sqrt{Z_o}}\right)\sqrt{4\, X_o\, Y_o}\ \frac{\alpha\beta}{\sqrt{(2\alpha^2 + \beta^2)}} \sin(2\pi\epsilon) \qquad (35)$$

in which the factors which may be varied are $(Z_1/\sqrt{Z_o})$ and $\alpha\beta/(2\alpha^2 + \beta^2)$. The factor $\sqrt{4\, X_o\, Y_o}$ is simply the square root of the area of the aperture limiting the fringes, so that this needs to be made as large as possible consistant with what tolerance conditions will allow.

If r is the ratio of the mark to space widths of the square wave grating, the Fourier coefficients Z_o and Z_1 are given by

$$Zo = \frac{1}{Po} \int_{-(\frac{r}{r+1})\frac{Po}{2}}^{+(\frac{r}{r+1})\frac{Po}{2}} dx = (\frac{r}{r+1})$$

$$Z_1 = \frac{1}{Po} \int_{-(\frac{r}{r+1})\frac{Po}{2}}^{+(\frac{r}{r+1})\frac{Po}{2}} e^{-i\frac{2\pi}{Po}x} dx = \frac{1}{\pi} \text{Sin } (\frac{r}{r+1})\pi$$

so that

$$\frac{Z_1}{\sqrt{Zo}} = \frac{\text{Sin}(\frac{r}{r+1})\pi}{\sqrt{(\frac{r}{r+1})}\pi}$$

and it is required to find the value of r which maximises this expression. The maximum occurs when

$$\frac{d}{dr} (\frac{Z_1}{\sqrt{Zo}}) = o$$

that is, when $t = (\frac{r}{r+1})\pi$ maximises $\frac{\text{Sin } t}{\sqrt{t}\sqrt{\pi}}$. This requires that

$$\frac{\sqrt{t} \text{ Cos } t - \text{Sin } t \frac{1}{2} \frac{1}{t}}{t} = 0$$

or $$t \text{ Cos } t = \frac{1}{2} \text{ Sin } t$$

that is when

$$\tan t = 2t.$$

This is turn occurs when

$$t = \left(\frac{r}{r+1}\right)\pi = 1.16$$

so that $r = 0.59$ is the optimum value for the mark to space ratio of the grating.

The remaining factor is $\alpha\beta/(2\alpha^2 + \beta^2)$ Now the original beam is split into two beams of amplitude α and one of amplitude β. Thus $(2\alpha^2 + \beta^2)$ is the total light flux and is constant, being determined by the luminance of the light source, and the geometry of the system. It is thus necessary to find the maximum value of the product $F(\alpha, \beta) = \alpha\beta$ subject to the condition that $2\alpha^2 + \beta^2 = k$, where k is a constant. Using the method of undetermined multipliers of Langrange, this requires the solution of the equations

$$F'_\alpha + \lambda \frac{\partial}{\partial \alpha}\left\{2\alpha^2 + \beta^2 - k\right\} = 0$$

$$F'_\beta + \lambda \frac{\partial}{\partial \beta}\left\{2\alpha^2 + \beta^2 - k\right\} = 0$$

or

$$\beta + \lambda\{4\alpha\} = 0$$

$$\alpha + \lambda\{2\beta\} = 0$$

From the second of these, the multiplier is given by $\lambda = \left(-\frac{\alpha}{2\beta}\right)$ so that the first becomes

$$\beta - \left(\frac{\alpha}{2\beta}\right) 4\alpha = 0$$

that is

$$\left(\frac{\beta}{\alpha}\right)^2 = 2$$

or $\beta = \sqrt{2}\ \alpha$. Thus the optimum ratio of the intensity of the third beam to that of (1) or (2) is 2.

Using the above optimum values for the signal to noise ratio, the ratio of the A.C. to the D.C. amplitudes is

$$\frac{F_1}{F_o} = 1{\cdot}12\ \mathrm{Sin}2\pi\epsilon$$

and, if a value $\frac{F_1}{F_o} = 0{\cdot}02$, is detectable, the precision of finding the path difference is

$$\delta p = \frac{\lambda}{350}$$

and for a double pass

$$\delta p = \frac{\lambda}{700}\ .$$

CHAPTER III

Reference has been made to the question of tilt errors in the third beam in Chapter II. The present chapter deals with these in more detail, and treats the question of the size of tilt errors which can be tolerated in the system. The effects of mismatch between the width of the aperture and the fringes, and between the fringe spacing and that of the grating, are also determined.

(1) Tolerances for the permissible tilt errors in the third beam.

Re-writing the expression for F_o and F_1 from Chapter II from (24), (27) and (29) we get

$$F_o = 4 Z_o X_o Y_o \left\{ (2\alpha^2 + \beta^2) + 2\alpha^2 \frac{\text{Sin}(2\pi\sigma X_o)}{(2\pi\sigma X_o)} + 2\alpha\beta \frac{\text{Sin}(2\pi VY_o)}{(2\pi VY_o)} \left[\frac{\text{Sin } 2\pi(\frac{\sigma}{2} + U)X_o}{2\pi(\frac{\sigma}{2} + U)X_o} + \frac{\text{Sin } 2\pi(\frac{\sigma}{2} - U)X_o}{2\pi(\frac{\sigma}{2} - U)X_o} \right] \text{Cos } kd \right\} \quad (1)$$

$$F_1 = 8 Z_1 X_o Y_o \left\{ (2\alpha^2 + \beta^2) \frac{\text{Sin}(2\pi\sigma_o X_o)}{(2\pi\sigma_o X_o)} + \alpha^2 \left[\frac{\text{Sin } 2\pi(\sigma - \sigma_o)X_o}{2\pi(\sigma - \sigma_o)X_o} + \frac{\text{Sin } 2\pi(\sigma + \sigma_o)X_o}{2\pi(\sigma + \sigma_o)X_o} \right] \right. \quad \text{Cont.}$$

Equation (2)
continued.

$$+\alpha\beta\,\frac{\mathrm{Sin}(2\pi\,VY_o)}{(2\pi\,VY_o)}\left[\left(\frac{\mathrm{Sin}\,2\pi\,(\frac{\sigma}{2}+U-\sigma_o)X_o}{2\pi\,(\frac{\sigma}{2}+U-\sigma_o)X_o}\right.\right.$$

$$\left.+\frac{\mathrm{Sin}\,2\pi\,(\frac{\sigma}{2}-U+\sigma_o)X_o}{2\pi\,(\frac{\sigma}{2}-U+\sigma_o)X_o}\right)e^{\,ikd} \qquad (2)$$

$$\left.+\left(\frac{\mathrm{Sin}\,2\pi\,(\frac{\sigma}{2}-U-\sigma_o)}{2\pi\,(\frac{\sigma}{2}-U-\sigma_o)}+\frac{\mathrm{Sin}\,2\pi\,(\frac{\sigma}{2}+U+\sigma_o)}{2\pi\,(\frac{\sigma}{2}+U+\sigma_o)}\right)e^{\,-ikd}\right]\Bigg\}$$

In expressions (10) and (11) we have a system with both the components of tilt error being non-zero. We proceed by assuming one of the component errors to be present in turn, with the others equal to zero. Fig. 1. (a) and (b) shows the situation with the tilt errors present separately.

(a) System with V-component of tilt error equal to zero.

As we are considering a system which is otherwise perfectly adjusted so we have from Chapter II

$$\sigma = 2\sigma_o$$

$$2\sigma X_o = N \qquad (3)$$

where σ and σ_o are the spatial frequencies of the fringes and of the grating respectively and N is the number of fringes in the length $2X_o$, N being assumed to be even. From (1), (2) and (3) we get,

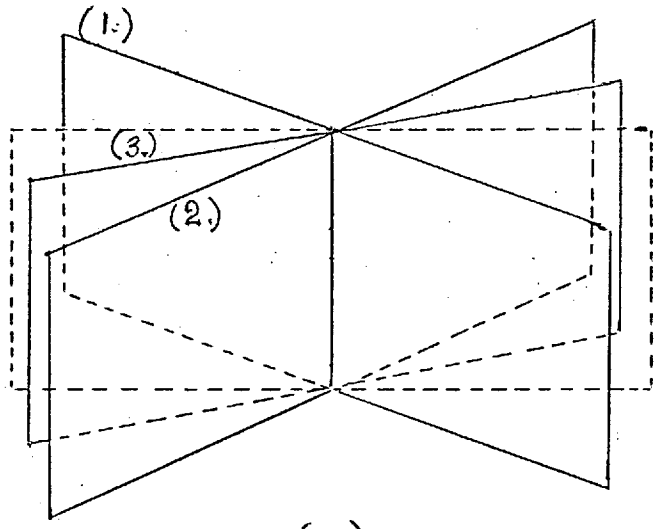

(a.)

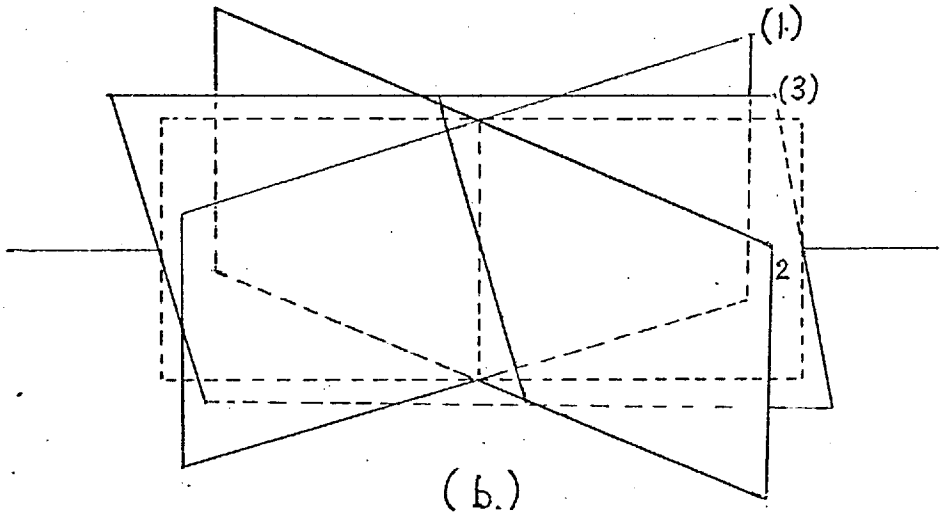

(b.)

Fig. 1.

Diagrammatic representation of the tilt-errors.

$$F_o = 4\, Z_o X_o Y_o \left\{ (2\alpha^2 + \beta^2) + 2\alpha^2 \frac{\mathrm{Sin}\,(N\pi)}{(N\pi)} \right.$$

$$+ 2\alpha\beta \left[\frac{\mathrm{Sin}\,(\frac{N}{2}\pi - 2\pi UX_o)}{(\frac{N}{2}\pi - 2\pi UX_o)} \right.$$

$$\left. \left. + \frac{\mathrm{Sin}\,(\frac{N}{2}\pi + 2\pi UX_o)}{(\frac{N}{2}\pi + 2\pi UX_o)} \right] \mathrm{Cos}\, kd. \right\} \qquad (4)$$

$$F_1 = 8 Z_1 X_o Y_o \left\{ (2\alpha^2 + \beta^2) \frac{\mathrm{Sin}\,\frac{N}{2}\pi}{\frac{N}{2}\pi} + \alpha^2 \left[\frac{\mathrm{Sin}\,\frac{N}{2}\pi +}{\frac{N}{2}\pi} \right.\right.$$

$$\left. \frac{\mathrm{Sin}\,(3\frac{N}{2}\pi)}{(3\frac{N}{2}\pi)} \right] + \alpha\beta \left[\left(\left(\frac{\mathrm{Sin}\,2\pi UX_o}{2\pi UX_o} + \right.\right.\right.$$

$$\left. \left. \frac{\mathrm{Sin}\,(N\pi - 2\pi UX_o)}{(N\pi - 2\pi UX_o)} \right) e^{ikd} + \left(\frac{\mathrm{Sin}\,(2\pi UX_o)}{(2\pi UX_o)} + \right. \right. \qquad (5)$$

$$\left. \left. \left. \frac{\mathrm{Sin}\,(N\pi + 2\pi UX_o)}{(N\pi + 2\pi UX_o)} \right) e^{-ikd} \right] \right\}$$

(4) and (5) on simplification and putting $\beta^2 = 2\alpha^2$ in the expression of F_o give,

$$F_o = 16\, Z_o X_o Y_o \alpha^2 \qquad (6)$$

$$F_1 = 16\, Z_1 X_o Y_o\, \alpha\beta\, \mathrm{Cos}\, kd\, \frac{\mathrm{Sin}\,(2\pi UX_o)}{(2\pi UX_o)} \qquad (7)$$

If the tilt error specified by U is other than zero, the A.C. signal is reduced, the new signal to noise ratio is proportional to,

$$\frac{\text{Signal}}{\text{Noise}} = \frac{F_1}{\sqrt{F_o}} = \frac{4Z_1}{Z_o}\sqrt{X_oY_o}\ \beta \text{ Cos kd } \frac{\text{Sin } 2\pi UX_o}{2\pi UX_o} \qquad (8)$$

which expression serves as a basis for the tolerance on the tilt error U. If in (8) $\frac{\text{Sin } (2\pi UX_o)}{(2\pi UX_o)} \leqq 0.9$,

the signal to noise ratio is not significantly affected. Then the maximum value of 'U' which can be tolerated for a given X_o (equal to 4.5 mm in the present case) in the system is about 50 seconds of arc.

(b) System with U-component of tilt error equal to zero

From expression (1), (2) for the present case when the U-component of the tilt error is zero, but V is non-zero, making substitutions from (3) we get F_o and F_1 as

$$F_o = 4Z_oX_oY_o\left\{(2\alpha^2+\beta^2) + 2\alpha^2\ \frac{\text{Sin } N\pi}{N\pi} + 4\alpha\beta\ \frac{\text{Sin } 2\pi VY_o}{2\pi VY_o}\ \frac{\text{Sin } \frac{N}{2}\pi}{\frac{N}{2}\pi}\ \text{Cos kd}\right\} \qquad (9)$$

$$F_1 = 8Z_1X_oY_o\left\{(2\alpha^2+\beta^2)\ \frac{\text{Sin } \frac{N}{2}\pi}{\frac{N}{2}\pi} + \alpha^2\left[\frac{\text{Sin } \frac{N}{2}\pi}{\frac{N}{2}\pi} + \frac{\text{Sin } \frac{3N}{2}\pi}{\frac{3N}{2}\pi}\right] + 2\alpha\beta\left(\frac{\text{Sin } 2\pi VY_o}{2\pi VY_o}\right)\left[1 + \frac{\text{Sin } N\pi}{N\pi}\right]\text{Cos kd}\right\} \qquad (10)$$

Simplifying (9) and (10) and putting $\beta^2 = 2\alpha^2$ in (9) we get

$$F_o = 16\, Z_o X_o Y_o\, \alpha^2 \qquad (11)$$

$$F_1 = 16\, Z_1 X_o Y_o\, \alpha\beta \cos kd\, \frac{\sin 2\pi VY_o}{2\pi VY_o} \qquad (12)$$

Again, a non-zero value of the tilt error reduces the A.C. signal and from (11) and (12) the new signal to noise ratio is found to be proportional to

$$\frac{\text{Signal}}{\text{Noise}} = \frac{F_1}{\sqrt{F_o}} = \frac{4Z_1}{\sqrt{Z_o}} \sqrt{X_o Y_o}\, \beta \cos kd\, \frac{\sin 2\pi VY_o}{2\pi VY_o} \qquad (13)$$

It may be noted that (13) is formally identical with (8), (UX_o) being merely replaoed by (VY_o). Again (13) serves as a basis for imposing a tolerance on the tilt error V. If in (13) $\frac{\sin (2\pi VY_o}{(2\pi VY_o)} \leq 0.9$, the signal to noise ratio is not significantly affected. Then the maximum value of 'U' which can be tolerated for a given Y_o (equal to 4 mm in the present case) in the system is about 45 seconds of arc.

(2) <u>The effect of mismatch of the fringe spacing to the grating</u>

In a system which is perfectly adjusted and where there is exact matching of the fringe spacing and the grating spacing the spatial frequency of the fringes is equal to exactly twice the spatial frequency of the grating: that is,

$$\sigma = 2\sigma_o$$

σ and σ_o being respectively the spatial frequencies of fringes and

grating. We will consider a system where there is a mis-match between the spacing of fringes and that of the grating. In this case the spatial frequency of the fringes may be written

$$\sigma' = \sigma + \delta\sigma \tag{14}$$

where σ is the spatial frequency, equal to $2\sigma_o$, giving perfect matching. Thus,

$$\sigma' = 2\sigma_o + \delta\sigma \tag{15}$$

From (3) we have,

$$2\sigma' X_o = N \tag{16}$$

for the number of fringes in the length $2X_o$. Let N_o be integral and equal to the number of grating periods in $2X_o$. Then, in the ideal conditions, $\sigma' = \sigma = 2\sigma_o$ and so,

$$N = 2N_o \tag{17}$$

and from (3) $N_o = 2\sigma_o X_o$. Rewriting the expressions for F_o, F_1, from (1) and (2) we have,

$$F_o = 4 Z_o X_o Y_o \left\{ (2\alpha^2 + \beta^2) + 2\alpha^2 \frac{\text{Sin } 2\pi\sigma' X_o}{2\pi\sigma' X_o} + 2\alpha\beta \frac{\text{Sin } 2\pi VY_o}{2\pi VY_o} \left[\frac{\text{Sin } 2\pi(\frac{\sigma'}{2} + U)X_o}{2\pi(\frac{\sigma'}{2} + U)X_o} + \frac{\text{Sin } 2\pi(\frac{\sigma'}{2} - U)X_o}{2\pi(\frac{\sigma'}{2} - U)X_o} \right] \text{Cos } kd \right\} \tag{18}$$

$$F_1 = 8 Z_1 X_o Y_o \left\{ (2\alpha^2 + \beta^2) \frac{\text{Sin } 2\pi\sigma X_o}{2\pi\sigma X_o} + \alpha^2 \left[\frac{\text{Sin } 2\pi(\sigma' - \sigma_o)X_o}{2\pi(\sigma' - \sigma_o)X_o} \right. \right.$$

$$+\frac{\operatorname{Sin} 2\pi(\sigma'+\sigma_o)X_o}{2\pi(\sigma'+\sigma_o)X_o}\Bigg] + \alpha\beta\,\frac{\operatorname{Sin} 2\pi VY_o}{2\pi VY_o}$$

$$\Bigg[\left(\frac{\operatorname{Sin} 2\pi(\frac{\sigma'}{2}+U-\sigma_o)X_o}{2\pi(\frac{\sigma'}{2}+U-\sigma_o)X_o} + \frac{\operatorname{Sin} 2\pi(\frac{\sigma'}{2}-U+\sigma_o)X_o}{2\pi(\frac{\sigma'}{2}-U+\sigma_o)X_o}\right) e^{ikd}$$

$$+\left(\frac{\operatorname{Sin} 2\pi(\frac{\sigma'}{2}-U-\sigma_o)X_o}{2\pi(\frac{\sigma'}{2}-U-\sigma_o)X_o} + \frac{\operatorname{Sin} 2\pi(\frac{\sigma'}{2}+U+\sigma_o)}{2\pi(\frac{\sigma'}{2}+U+\sigma_o)}\right) e^{-ikd}\Bigg]\Bigg\} \quad (19)$$

Using (14), (15), (16), (17) in (18) and (19), these formulae reduce to

$$F_o = 4\,Z_oX_oY_o\left\{(2\alpha^2+\beta^2) + 2\alpha^2\,\frac{\operatorname{Sin} N\pi + 2\pi\delta\sigma X_o}{N\pi + 2\pi\delta\sigma X_o}\right.$$

$$\left. + (-)^{\frac{N}{2}}\,4\alpha\beta\left[\frac{\operatorname{Sin}\frac{N}{2}\pi+\pi\delta\sigma X_o}{\frac{N}{2}\pi+\pi\delta\sigma X_o}\right]\operatorname{Cos} kd\right\} \quad (20)$$

and,

$$F_1 = 8\,Z_1X_oY_o\left\{(2\alpha^2+\beta^2)\,\frac{\operatorname{Sin}\frac{N}{2}\pi}{\frac{N}{2}\pi} + \right.$$

$$\alpha^2\left[\frac{\operatorname{Sin}\frac{N}{2}\pi + 2\pi\delta\sigma X_o}{\frac{N}{2}\pi + 2\pi\delta\sigma X_o} + \frac{\operatorname{Sin}\frac{3N}{2}\pi + 2\pi\delta\sigma X_o}{\frac{3N}{2}\pi + 2\pi\delta\sigma X_o}\right]$$

$$\left. + 2\alpha\beta\left[\frac{\operatorname{Sin}(\pi\delta\sigma X_o)}{(\pi\delta\sigma X_o)} + \frac{\operatorname{Sin}(N\pi+\pi\delta\sigma X_o)}{(N\pi+\pi\delta\sigma X_o)}\right]\operatorname{Cos} kd\right\} \quad (21)$$

respectively: (20) and (21) may be further simplified, and putting $\beta^2 = 2\alpha^2$ in (19) then gives,

$$F_o = 16\, Z_o X_o Y_o \alpha^2 \tag{22}$$

$$F_1 = 16\, Z_1 X_o Y_o\, \alpha\beta \;\; \text{Cos kd} \;\; \frac{\text{Sin}(\pi\delta\sigma X_o)}{(\pi\delta\sigma X_o)} \tag{23}$$

From (22) and (23) we get the signal to noise ratio being proportional to,

$$\frac{\text{Signal}}{\text{Noise}} = \frac{F_1}{\sqrt{F_o}} = \frac{4Z_1}{\sqrt{Z_o}} \sqrt{X_o Y_o}\, \beta \;\; \text{Cos kd} \;\; \frac{\text{Sin}\,(\pi\,\delta\sigma X_o)}{(\pi\delta\sigma X_o)} \tag{24}$$

Again, from (24), the effect of this error is seen to be to reduce the strength of the A.C. signal.

(3) <u>The effect of mismatch between the width of the aperture and fringes.</u>

It is now assumed that the system is free from tilt errors and also that the spatial frequencies of the fringes and of the grating are perfectly matched. Let us suppose, however, that the width of the aperture is not exactly equal to a whole number of periods of the grating. That is the length $2X_o$ is now represented by $2(X_o + \delta X_o)$, where $2\delta X_o$ is the error in the width of the aperture. Write then

$$X_o' = X_o + \delta X_o \tag{25}$$

From (3) we have

$$2\sigma X_o' = N$$

$$2\sigma_o X_o' = N_o \tag{26}$$

$$\sigma = 2\sigma_o$$

Substituting now from (18), (19), (25) and (26) and remembering that X_o in (18) and (19) is replaced by X_o', we get

$$F_o = 4Z_o(X_o + \delta X_o)Y_o \left\{(2\alpha^2 + \beta^2) + 2\alpha^2 \frac{\mathrm{Sin}(N\pi + 2\pi\sigma\delta X_o)}{(N\pi + 2\pi\sigma\delta X_o)} + 4\alpha\beta\left[\frac{\mathrm{Sin}(\frac{N}{2}\pi + \pi\delta X_o\sigma)}{(\frac{N}{2}\pi + \pi\delta X_o\sigma)}\right]\mathrm{Cos}\ kd\right\} \quad (27)$$

$$F_1 = 8Z_1(X_o + \delta X_o)Y_o \left\{(2\alpha^2 + \beta^2)\frac{\mathrm{Sin}(N_o\pi + 2\pi\sigma_o\delta X_o)}{(N_o\pi + 2\pi\sigma_o\delta X_o)} + \alpha^2\left[\frac{\mathrm{Sin}(N_o\pi + 2\pi\sigma_o\delta X_o)}{(N_o\pi + 2\pi\sigma_o\delta X_o)} + \frac{\mathrm{Sin}(3N_o\pi + 3.2\pi\sigma_o\delta X_o)}{(3N_o\pi + 3.2\pi\sigma_o\delta X_o)}\right] + 2\alpha\beta\left[1 + \frac{\mathrm{Sin}(2\pi N_o + 4\pi\sigma_o\delta X_o)}{(2N_o\pi + 4\pi\sigma_o\delta X_o)}\right]\mathrm{Cos}\ kd\right\} \quad (28)$$

Expressions (27) and (28) on simplification, and putting $\beta^2 = 2\alpha^2$ in (27) and $d = (\epsilon - \frac{1}{4})\lambda$ (as in Chapter II), give

$$F_o = 16\alpha^2 Y_o Z_o (X_o + \delta X_o) \quad (29)$$

$$F_1 = 8Z_1(X_o + \delta X_o)Y_o\,\alpha^2 \left\{5(-1)^{N_o}\frac{\mathrm{Sin}(2\pi\sigma_o\delta X_o)}{(N_o 2\pi\sigma_o\delta X_o)} + (-1)^{N_o}\frac{\mathrm{Sin}(3.2\pi\sigma_o\delta X_o)}{(3N_o\pi + 3.2\pi\sigma_o\delta X_o)} + 2.84\,\mathrm{Sin}2\pi\epsilon\right\} \quad (30)$$

From (29) and (30) the signal to noise ratio is,

$$\frac{\text{Signal}}{\text{Noise}} = \frac{F_1}{\sqrt{F_o}} = \frac{2Z_1\sqrt{Y_o}}{\sqrt{Z_o}}\ \alpha\sqrt{X_o + \delta X_o}\left\{\frac{5(-1)^{N_o}\ \text{Sin}\ 2\pi\sigma_o\delta X_o}{N_o\pi + 2\pi\sigma_o\delta X_o}\right.$$

$$+\frac{(-1)^{N_o}\ \text{Sin}(3.2\pi\ \sigma_o\delta X_o)}{(3N_o\pi\ + 3.2\pi\sigma_o\delta X_o)}$$

$$\left. + 2.84\ \text{Sin}\ 2\pi\epsilon\right\} \qquad (31)$$

Signal to noise ratio is maximum for $\delta X_o = o$ (31) then gives,

$$\frac{\text{Signal}}{\text{Noise}} = \frac{F_1}{\sqrt{F_o}} = \frac{5.68\ Z_1}{\sqrt{Z_o}}\sqrt{X_oY_o}\ \alpha\quad \text{Sin}\ 2\pi\epsilon \qquad (32)$$

For δX_o small (31) gives

$$\frac{\text{Signal}}{\text{Noise}} = \frac{F_1}{\sqrt{F_o}} = \frac{2Z_1}{\sqrt{Z_o}}\ \sqrt{Y_o}\ \alpha\ \sqrt{X_o}\left(1 + \frac{\delta X_o}{2X_o}\right)\Bigg[$$

$$5(-1)^{N_o}\ \frac{2\pi\sigma_o\delta X_o}{N_o\pi} + (-1)^{N_o}\ \frac{6\pi\sigma_o\delta X_o}{3N_o\pi}$$

$$+ 2.84\ \text{Sin}\ 2\pi\epsilon\Bigg] \qquad (33)$$

(33) on simplification and putting $2X_o = \frac{N_o}{\sigma_o}$ ..gives,

$$\frac{\text{Signal}}{\text{Noise}} = \frac{F_1}{\sqrt{F_o}} = \frac{12\ \sigma_o\ \delta X_o}{N_o} + \frac{2.84\ \sigma_o\ \delta X_o}{N_o}\ \text{Sin}2\pi\epsilon + 2.84\text{Sin}\ 2\pi$$

$$\frac{\text{Signal}}{\text{Noise}} = \frac{12\sigma_o\delta X_o}{N_o} + \frac{0.09\ \sigma_o\ \delta X_o}{N_o} + 2.84\ \text{Sin}\ 2\pi\epsilon$$

$$\frac{F_1}{\sqrt{F_o}} = \frac{12.09\ \sigma_o\ \delta X_o}{N_o} + 2.84\ \text{Sin}\ 2\pi\epsilon \qquad (34)$$

From (34) we get,

$$\left| \frac{12.09\ \sigma_o\ \delta\ X_o}{N_o} \right| << \quad 2.84\ \text{Sin}\ 2\pi\epsilon \qquad (35)$$

Substituting $N_o = 2\ \sigma_o X_o$, putting $X_o = 4.5$ mm and Sin $2\pi\epsilon$ (from Chapter II) = 0.032 we get,

$$\delta X_o < 0.06 \text{ mm.}$$

CHAPTER IV

(a) Spatial Coherence and 3-beam Fringes

Fig. I shows schematically the general arrangement of a three-beam interferometer. Light from a small source proceeds by way of the arms (1), (2) and (3) to produce fringes in the plane at P. Conjugate object points P_1, P_2 and P_3 are found in the source space such that P is the image of P_1 formed by light traversing arm (1), P_2 similarly is the object point which is imaged at P along arm (2) and P_3 is the object point which is imaged at P along arm (3). Let an element ds of the source produce complex amplitudes U_1, U_2 and U_3 at P_1, P_2 and P_3 respectively. If f_1, f_2 and f_3 are the complex transmissions for the paths P_1 to P, P_2 to P and P_3 to P, then the total complex amplitude at P is given by the sum,

$$f_1U_1 + f_2U_2 + f_3U_3 \qquad (1)$$

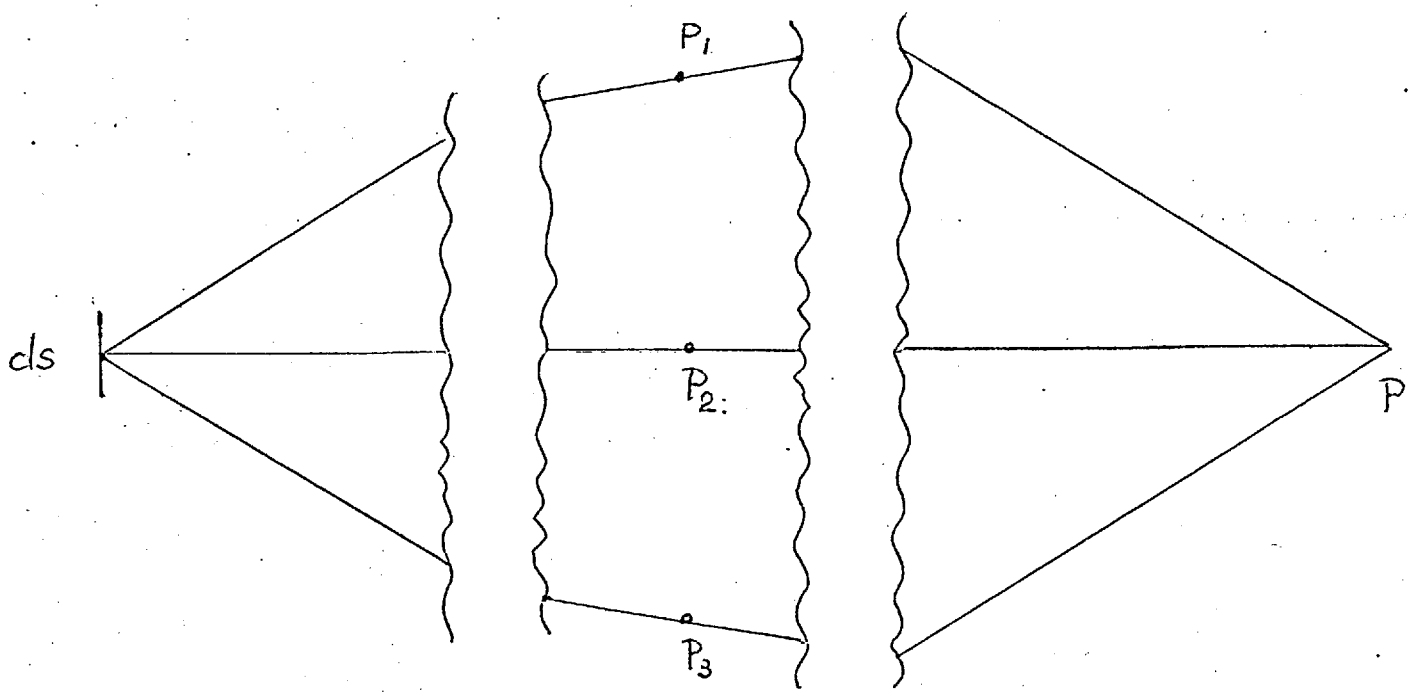

Fig. 1.

The intensity due to ds at P is then

$$|f_1U_1 + f_2U_2 + f_3U_3|^2 \, ds \tag{2}$$

Total intensity at P due to whole of the source is given by

$$I_P = \iint_S |f_1U_1 + f_2U_2 + f_3U_3|^2 \, ds \tag{3}$$

Expanding the brackets in (3) and noting that

$$\begin{aligned} I_1 &= \iint_S |U_1|^2 \, ds \\ I_2 &= \iint_S |U_2|^2 \, ds \\ I_3 &= \iint_S |U_3|^2 \, ds \end{aligned} \tag{4}$$

we get the expression for the total intensity at P due to whole of the source as,

$$\begin{aligned} I_P = {} & |f_1|^2 I_1 + |f_2|^2 I_2 + |f_3|^2 I_3 \\ & + \iint_S 2\mathrm{Re}\{U_1^* U_2 f_1^* f_2\} \, ds \\ & + \iint_S 2\mathrm{Re}\{U_2^* U_3 f_2^* f_3\} \, ds \\ & + \iint_S 2\mathrm{Re}\{U_3^* U_1 f_3^* f_1\} \, ds \end{aligned} \tag{5}$$

In (5) I_1, I_2 and I_3 represent the separate intensities at P_1, P_2 and P_3 due to whole of the source. The sign * in (5) denotes the complex conjugate. The degrees of coherence between the points P_1, P_2 and P_3, taken in pairs are defined by,

$$\Gamma_{21} = \frac{1}{\sqrt{I_1 I_2}} \iint_S U_1^* U_2 ds$$

$$\Gamma_{32} = \frac{1}{\sqrt{I_2 I_3}} \iint_S U_2^* U_3 ds \qquad (6)$$

$$\Gamma_{13} = \frac{1}{\sqrt{I_3 I_1}} \iint_S U_3^* U_1 ds$$

and thus, using (6) in (5), the latter becomes,

$$\begin{aligned} I_p = {} & |f_1|^2 I_1 + |f_2|^2 I_2 + |f_3|^2 I_3 \\ & + 2\sqrt{I_1 I_2}\, \mathrm{Re}(\Gamma_{21} f_1^* f_2) \\ & + 2\sqrt{I_2 I_3}\, \mathrm{Re}(\Gamma_{32} f_2^* f_3) \\ & + 2\sqrt{I_3 I_1}\, \mathrm{Re}(\Gamma_{13} f_3^* f_1) \end{aligned} \qquad (7)$$

As f_1 is the complex amplitude produced at P by a wave of unit amplitude and zero phase at P_1 therefore,

$$f_1 = |f_1| \exp(i\Phi_1)$$

Similarly,

$$\begin{aligned} f_2 &= |f_2| \exp(i\Phi_2) \\ f_3 &= |f_3| \exp(i\Phi_3) \end{aligned} \qquad (8)$$

In expression (8)

$$\begin{aligned} \Phi_1 &= (\text{phase at P}) - (\text{phase at } P_1) \\ \Phi_2 &= (\text{phase at P}) - (\text{phase at } P_2) \\ \Phi_3 &= (\text{phase at P}) - (\text{phase at } P_3) \end{aligned} \qquad (9)$$

Also if I_1', I_2' and I_3' are the separate intensities produced at

P then

$$I_1' = |f_1|^2 I_1$$
$$I_2' = |f_2|^2 I_2 \qquad (10)$$
$$I_3' = |f_3|^2 I_3$$

From (7), (8) and (10) we get

$$Ip = I_1' + I_2' + I_3' + 2\sqrt{I_1' I_2'}\,\mathrm{Re}(\Gamma_{21} e^{i(\Phi_2 - \Phi_1)})$$
$$+2\sqrt{I_2' I_3'}\,\mathrm{Re}(\Gamma_{32} e^{i(\Phi_3 - \Phi_2)}) \qquad (11)$$
$$+2\sqrt{I_3' I_1'}\,\mathrm{Re}(\Gamma_{13} e^{i(\Phi_1 - \Phi_3)})$$

From (6) and (8) we can say that $\Gamma_{21}, \Gamma_{32}, \Gamma_{13}$ respectively are determined by the degree to which the phase differences between $(P_2, P_1), (P_3, P_2), (P_1, P_3)$, varys for light from different points of the source. In the general case

$$\Gamma_{21} = V_{21} e^{i\beta_{21}}$$
$$\Gamma_{32} = V_{32} e^{i\beta_{32}} \qquad (12)$$
$$\Gamma_{13} = V_{13} e^{i\beta_{13}}$$

From (11) and (12) we now get

$$Ip = I_1' + I_2' + I_3' + 2V_{21}\sqrt{I_1' I_2'}\,\mathrm{Cos}\left[(\Phi_2 - \Phi_1) + \beta_{21}\right]$$
$$+ 2V_{32}\sqrt{I_2' I_3'}\,\mathrm{Cos}\left[(\Phi_3 - \Phi_2) + \beta_{32}\right] \qquad (13)$$
$$+ 2V_{13}\sqrt{I_3' I_1'}\,\mathrm{Cos}\left[(\Phi_1 - \Phi_3) + \beta_{13}\right]$$

(13) gives the general expression for the intensity in the fringe plane. In order to investigate the effect of the introduction of the third beam on the two-beam fringe system formed by light beams from the cube we proceed in the manner given below.

Fig. 2 shows schematically the three beam interferometer. The plane of best contrast of the two-beam fringes is at the reflecting faces of the cube interferometer and this is re-imaged at a convenient position by the lens F_1. P_1 and P_2 are coincident (in the case of two-beam fringes) and so $\Gamma_{21} = 1$. This means that the visibility remains high even for larger source sizes. (13) gives the general expression for the intensity in the fringe plane. To find an expression for the intensity of two-beam fringes we put;

$$\begin{aligned} I_3' &= 0 \\ \phi_2 &= -\phi_1 = \frac{2\pi}{\lambda} x\theta \end{aligned} \qquad (14)$$

In (14) x and θ respectively represent the distance in the fringe plane and the tilt. (13) and (14) give,

$$I_p = I_1' + I_2' + 2\sqrt{I_1' I_2'} \cos\left(\frac{4\pi}{\lambda} x\theta\right) \qquad (15)$$

The varying part of (15) is diagrammatically represented by Fig. 3. (15) gives the intensity of the fringes in case of the two-beam fringes. Let now the third beam be introduced. In order to get the expression for the distribution of intensity in this case let:

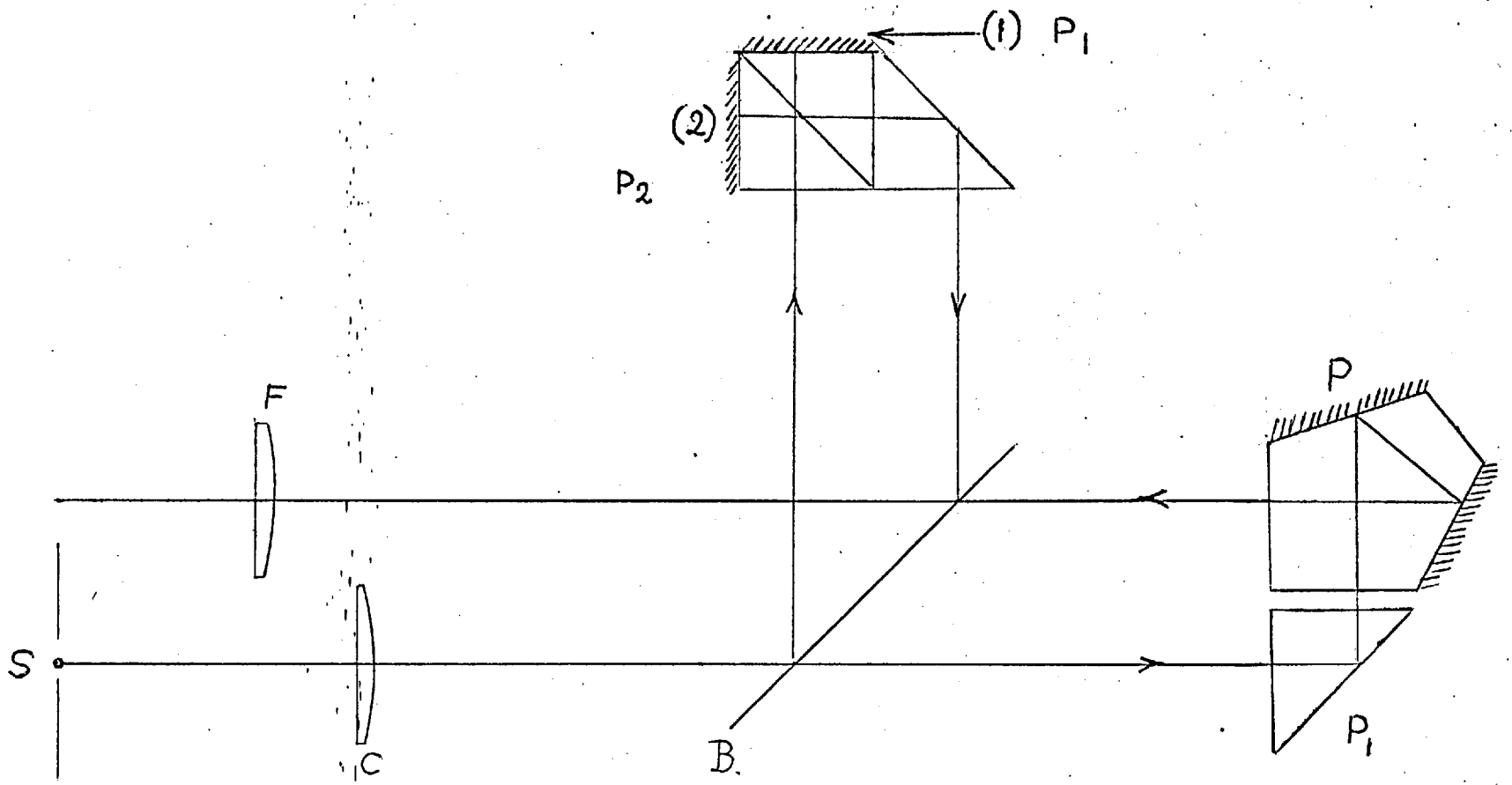

Fig. 2

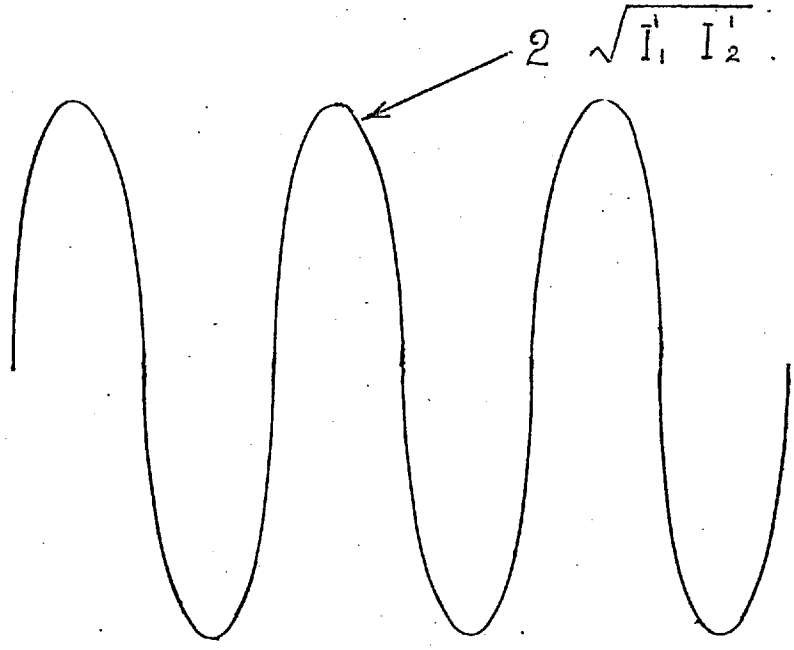
$2\sqrt{I_1' I_2'} \cdot \cos\left(\frac{4\pi}{\lambda} \cdot x \cdot \theta\right)$

Fig. 3.

$$\phi_3 = \frac{\pi}{2} - \epsilon$$

$$\Gamma_{13} = \Gamma_{32} = \Gamma = V \cdot \exp(i\beta) \tag{16}$$

From (13), (14) and (15) we get

$$Ip = I_1' + I_2' + I_3' + 2\sqrt{I_1' I_2'}\ \mathrm{Cos}\left(\frac{4\pi}{\lambda} x\, \theta\right) + 2V\sqrt{I_2' I_3'}\ \mathrm{Sin}\left[\frac{2\pi}{\lambda}\theta x + (\epsilon - \beta)\right] - 2V\sqrt{I_3' I_1'}\ \mathrm{Sin}\left[\frac{2\pi}{\lambda}\theta x - (\epsilon - \beta)\right] \tag{17}$$

Let us consider the case when $I_1' = I_2' = I'$. This gives:

$$Ip = 2I' + I_3' + 2I'\ \mathrm{Cos}\left(\frac{4\pi}{\lambda} x\theta\right) + 4V\sqrt{I' I_3'}\ \mathrm{Cos}\frac{2\pi}{\lambda}\theta x\ \mathrm{Sin}\left(\frac{\epsilon - \beta}{2}\right) \tag{18}$$

(18) shows that the effect produced by β, the argument of Γ_{13}, is to shift the zero of ϵ. Fig. 4 represents (18) graphically Given a symmetrically shaped small source, β is expected to be zero. Assuming this to be so, the effect of the third beam on the two-beam fringes is seen to be to introduce an additional D.C. term and also a term of spatial frequency equal to one half that of the two-beam fringes. Thus alternate fringes of the two-beam system will appear to be increased and decreased respectively in intensity. The scanning grating has a fundamental spatial frequency component introduced by the third beam. In perfect adjustment the scanning will, therefore, detect on the presence of the new component, whose amplitude is proportional to $\mathrm{Sin}\ \frac{\epsilon}{2}$

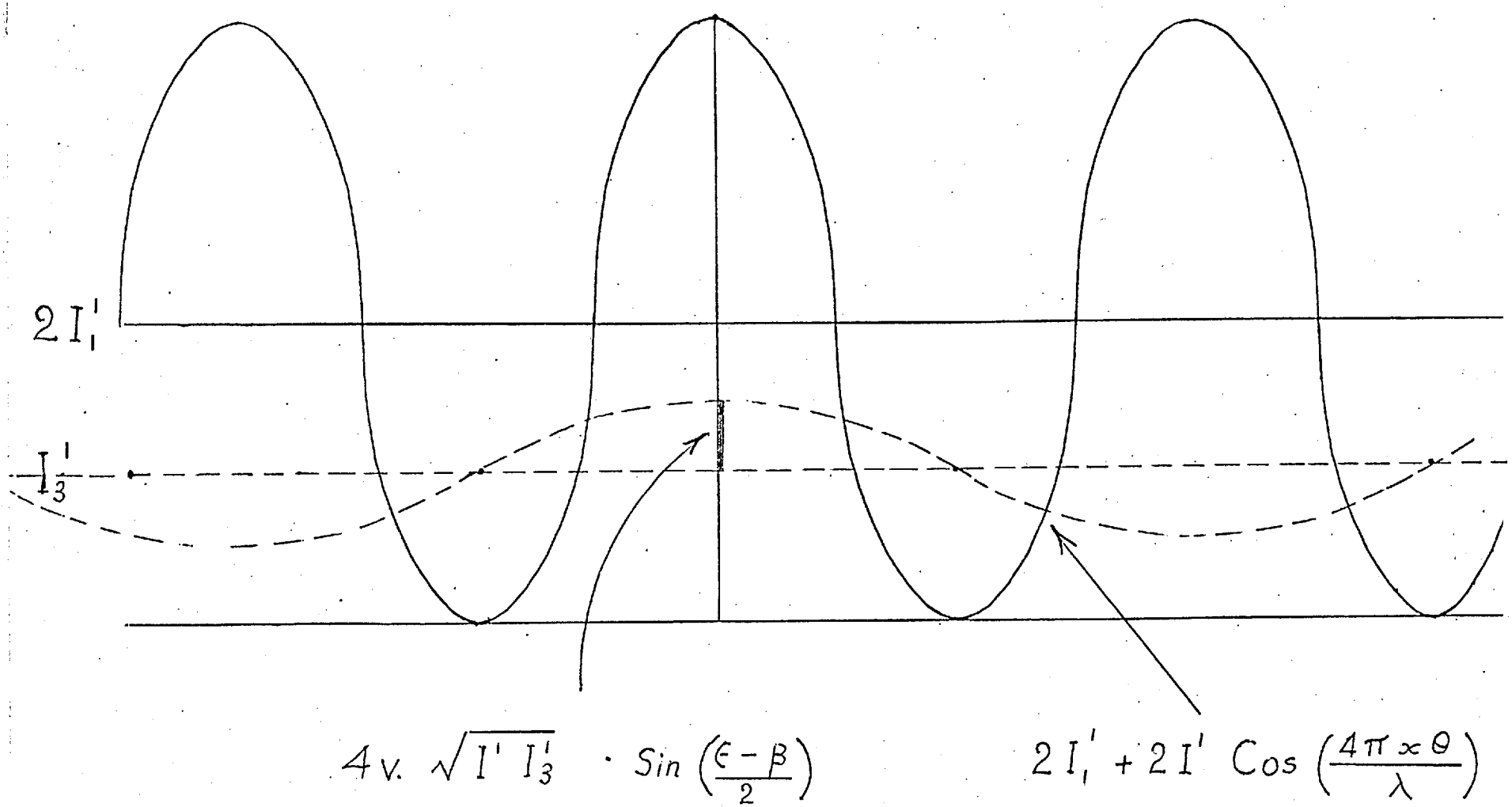
$2I_1'$
I_3'
$4v.\sqrt{I'\,I_3'}\cdot \sin\left(\frac{\epsilon-\beta}{2}\right)$
$2I_1' + 2I'\cos\left(\frac{4\pi x\theta}{\lambda}\right)$

Fig. 4.

Tolerance on the source size

Fig. 2 represents schematically the three-beam interferometer which we propose to study. In order to find the tolerance on the source size we re-draw the diagram as is shown by Fig. 5. In order to find the points P_{12} and P_3, images Q_{12} and Q_3 of Q_1 in the reflecting surfaces of arms (1) and (2) are found as is shown in Fig. 5, and then P_{12}, P_3 are the object points in the source space c conjugate to Q_{12}, Q_3. C is here the collimating lens. Q_{12} is the image of Q formed by the reflecting surfaces P_1, P_2 of the cube. Let F be the focal length of the field lens C' and let D denote the distance between F and T'. (Fig. 5). T' represents the reflecting surface in the arm (1). Further let d be the distance of the object point Q from T'. Also if R represents the reflecting surface in the arm (2) then let RT' = t. As Q_{12} Q_3 are the images of Q formed by the reflecting surfaces in arm (1) and (2) their distances from the front focus of C' will be (D - d) and (D - d - 2t) respectively. C' is considered here as a mirror image of C. Applying Newton's conjugate relation for C' we get

$$(D - d)\,\bar{R}_1 = F^2$$
$$(D - d - 2t)\,\bar{R}_2 = F^2 \qquad (19)$$

From (19) we get,

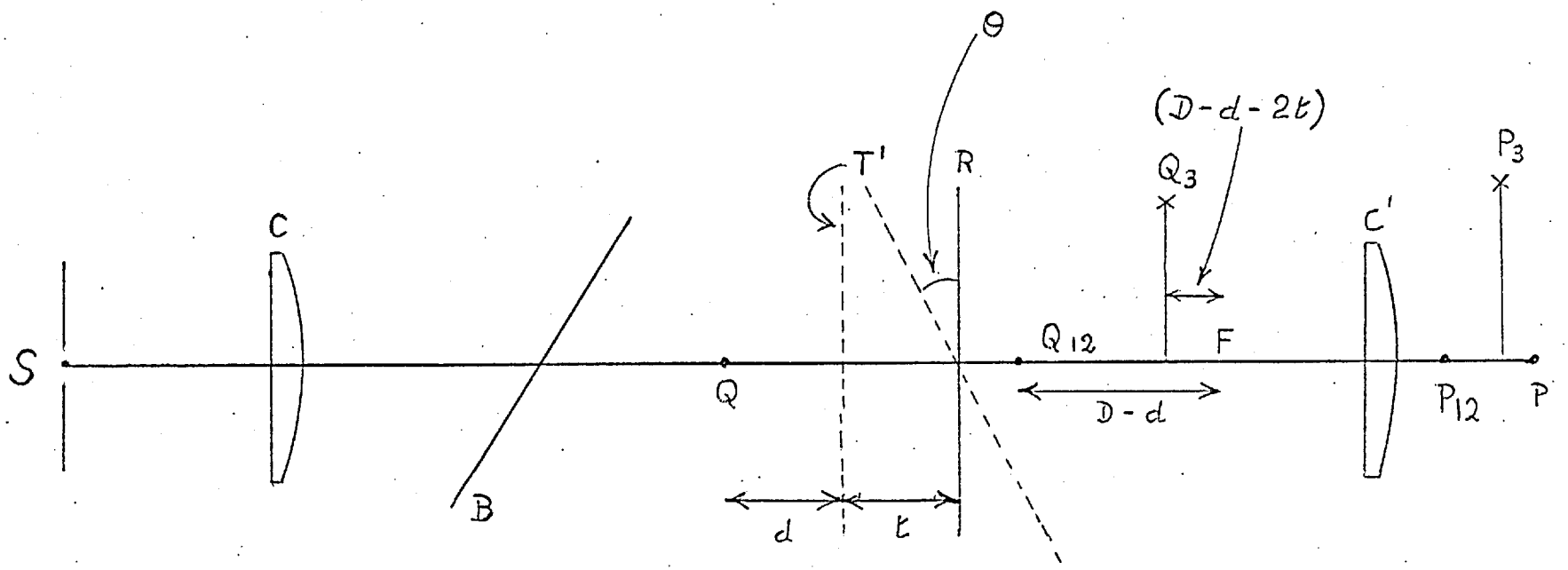

Fig. 5.

$$\bar{R}_1 = \frac{F^2}{(D-d)}$$
$$\bar{R}_2 = \frac{F^2}{(D-d-2t)} \qquad (20)$$

$\bar{R}_1$ and $\bar{R}_2$ in (20) represent respectively the distance of P_{12} and P_3 (the object points in the source space), from the focal plane of the lens C .

It can be shown, that for the maximum size of the source giving a contrast $\geqq$ 0.80 we have the expression: (ref. to H.H. Hopkins Advanced Optical Techniques, Chapter 6).

$$\Omega = \left(\frac{\pi}{\lambda}\right)^2 \left[\frac{1}{3} A^2 \sigma^4 + B^2 \sigma^2\right] \leqq 0.4 \qquad (21)$$

In (21) σ is the source radius and A, B are defined by the expression,

$$A = \frac{1}{2} \left(\frac{1}{\bar{R}_1} - \frac{1}{\bar{R}_2}\right) \qquad (22)$$

$$B = \sqrt{\left[(\alpha_2 - \alpha_1)^2 + (\beta_2 - \beta_1)^2\right]} \qquad (23)$$

$\bar{R}_1$ and $\bar{R}_2$ in (22) are defined by (19) and (20). Also $\alpha_1, \beta_1, \alpha_2, \beta_2$ are the direction cosines of $P P_{12}$ and $P P_3$. From (19) and (20) we have,

$$A = \frac{t}{F^2} \qquad (24)$$

The point P_{12} lies on the axis so $\alpha_1 = \beta_1 = o$. The distance of Q_3 from the axis is $2(d + t)\Theta$. (Fig.5) where Θ is the tilt of R (third beam). In order to find the value of α_2 the angle which P_3 makes with the axis we make use of the magnification relation which gives us,

$$\alpha_2 = \frac{2(d + t)\Theta}{F} \tag{25}$$

From (23) and (25) we get

$$B = \frac{2(d + t)\Theta}{F} \tag{26}$$

Re-writing (21) we have

$$\Omega = \left(\frac{\pi}{\lambda}\right)^2 \left[\frac{1}{3} A^2 \sigma^4 + B^2 \sigma^2\right] \leqq 0.4$$

From this we can also write

$$\left(\frac{\pi}{\lambda}\right)^2 \frac{1}{3} A^2 \sigma^4 \leqq 0.20 \tag{27}$$

$$\left(\frac{\pi}{\lambda}\right)^2 B^2 \sigma^2 \leqq 0.20 \tag{28}$$

we can write (27) and (28) as

$$\sigma_t = 4\sqrt{\frac{3 \times 0.20\ \lambda^2}{\pi^2 A^2}} \tag{29}$$

$$\sigma_\Theta = \sqrt{0.20}\ \frac{\lambda}{\pi B} \tag{30}$$

(29) and (30) would give tolerances with respect to path difference 't' and tilt 'Θ'. Substituting for A and B in (29) and (30) we get

$$\frac{\sigma_t}{F} = 4\sqrt{0.60}\sqrt{\frac{\lambda}{\pi t}} \tag{31}$$

$$\frac{\sigma_\theta}{F} = \frac{1}{2}\sqrt{0.20}\;\frac{\lambda}{\pi(t+d)\theta} \qquad (32)$$

If we take $t = 1$ mm, $\theta = 0.0003$, $d = 1$ mm, and $\lambda = 0.0005$ mm then we get,

$$\frac{\sigma_t}{F} \approx 37'$$

$$\frac{\sigma_o}{F} \approx 3^\circ$$

The size of pinhole used as the source was chosen to be $\sigma = 0.27$ mm giving $\frac{\sigma}{F} \approx 3'$ ($F = 12$ inches).

CHAPTER V

(1) Introduction

This chapter describes constructional details of the three-beam interferometer, the general arrangement of which is shown schematically in Fig. 1.

A more detailed diagram of the interferometer is shown by Fig. 2. This arrangement has a number of advantages, of particular importance being the equality of the amplitudes of beams and that the system lends itself well to the use of photo-electric detection These are matters that were discussed earlier, in Chapter I and Chapter II.

With these general remarks, we may proceed to describe each component in detail.

(2) Illuminating System

The illuminating system consists of a Philips low pressure mercury lamp rated at 125 watts, supplied from a Philips leak transformer, type L 4140. The mercury lamp is enclosed in a lamp house, the emergent light passing through a condensing lens G_1 and a field lens G_2 falls on the pin-hole of radius 0.26 mm. The pin-hole is at the focus of a collimating lens, which is a doublet lens of 12 inches focal length. A wratten No. 77 filter is placed between the pin-hole and the collimating lens which isolates 5461 ^{o}A line of the mercury spectrum. The light from the collimating lens is limited by a square aperture.

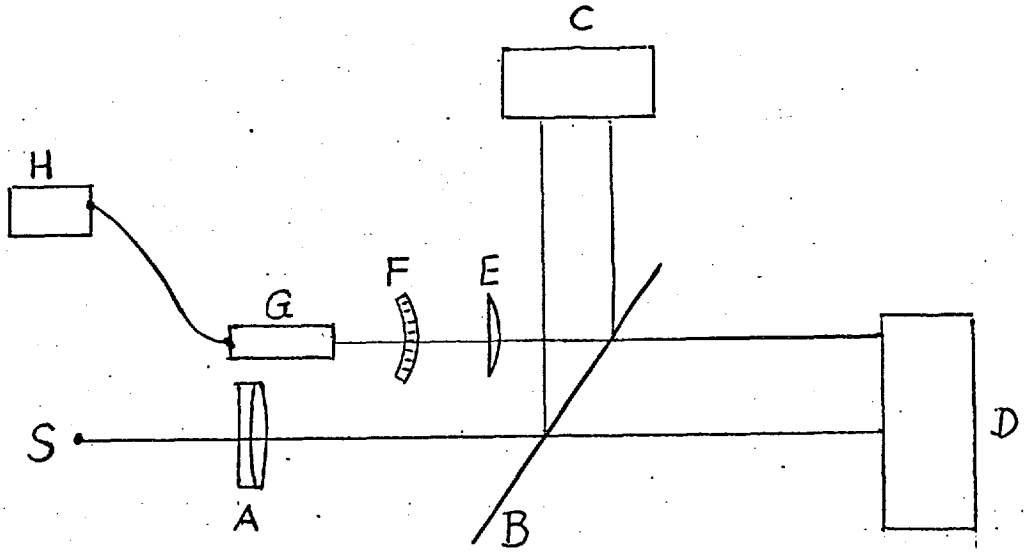

Fig. 1.

S Source.

A Collimating Lens.

B Beam-splitter.

C Cube and prism combination.

D Pentagonal prism and prism combination.

E Field lens.

F Radial grating.

G Photomultiplier.

H Synchronous Amplifier.

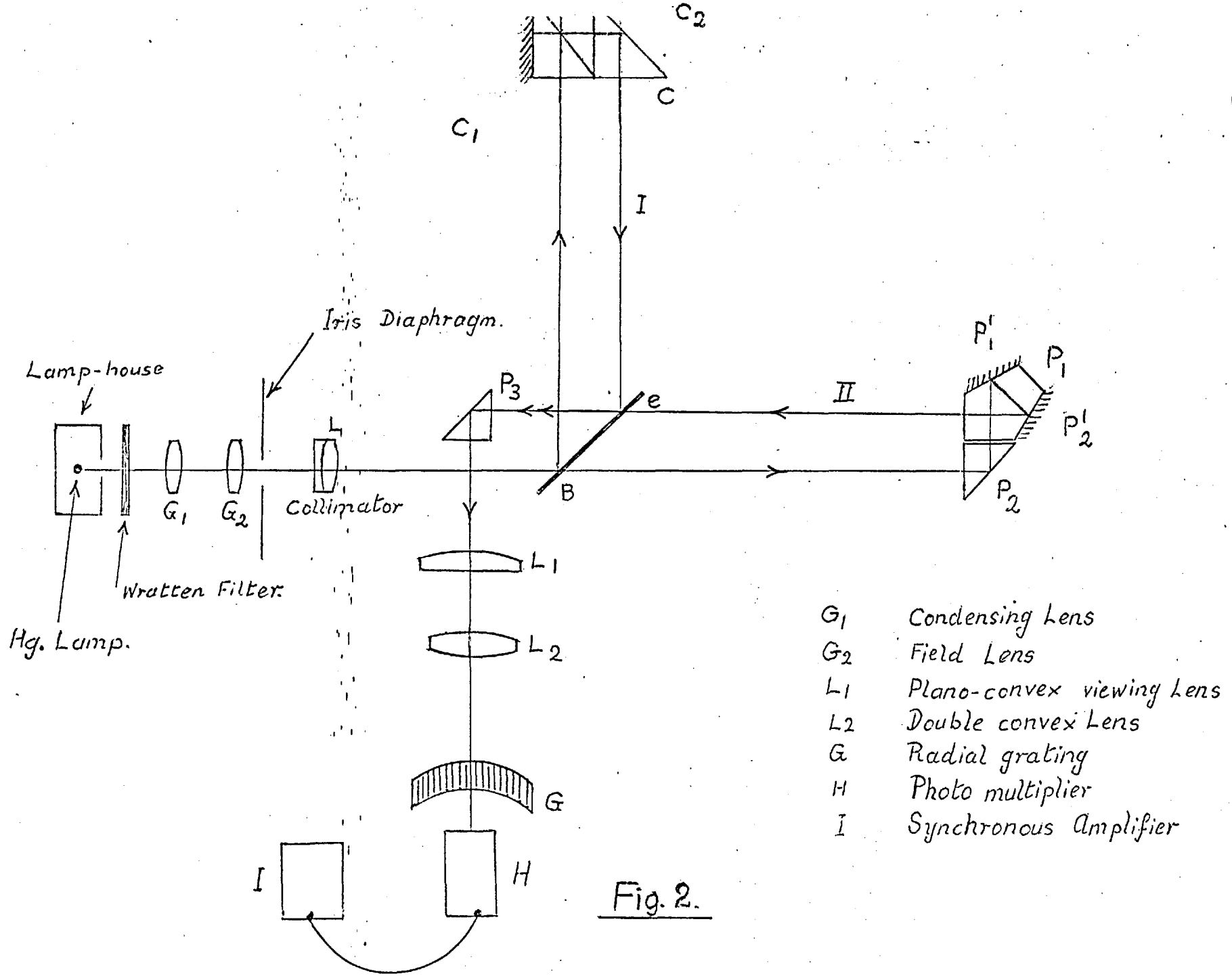

Fig. 2.

G_1	Condensing Lens
G_2	Field Lens
L_1	Plano-convex viewing Lens
L_2	Double convex Lens
G	Radial grating
H	Photo multiplier
I	Synchronous Amplifier

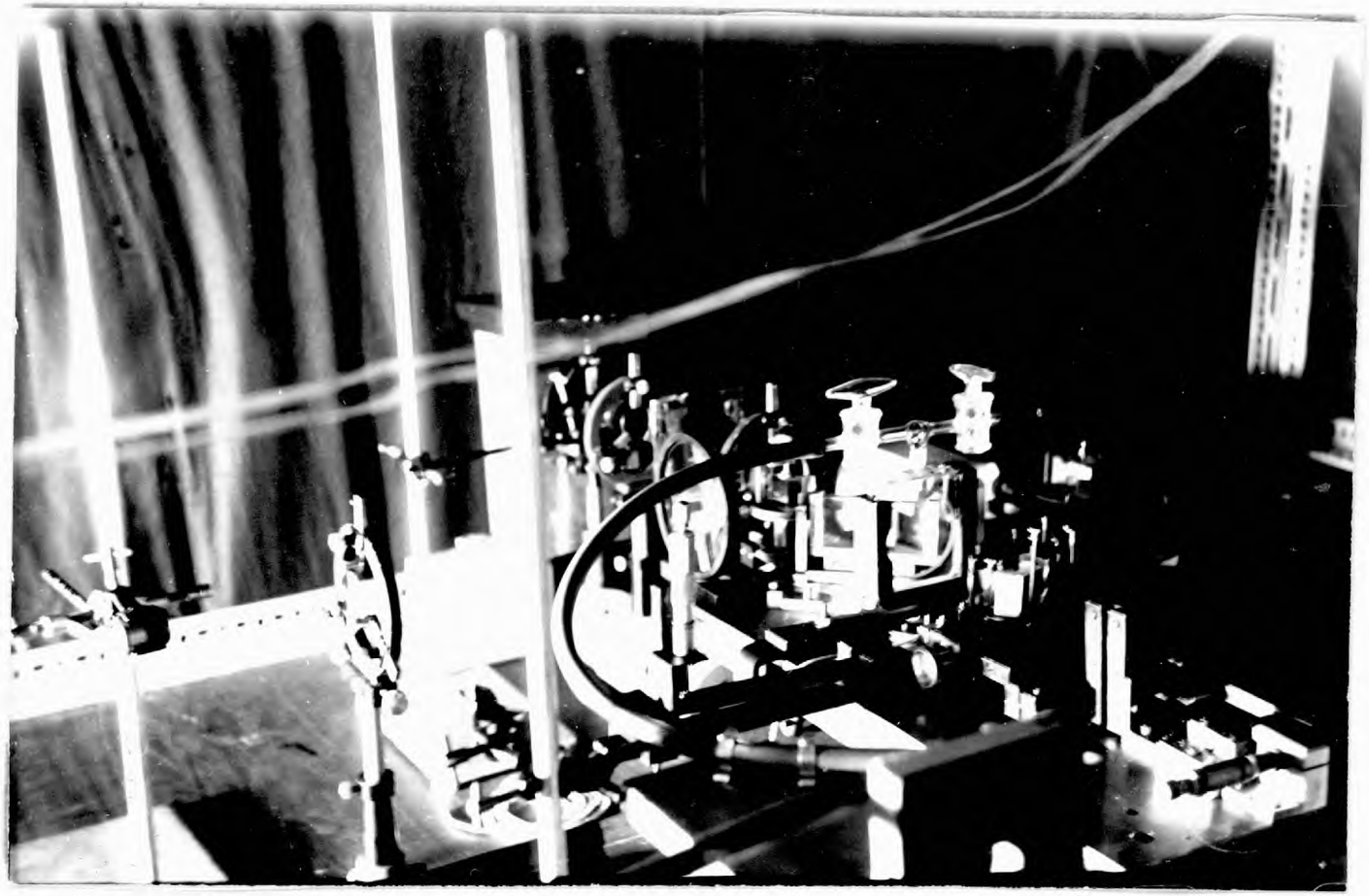

Plate I - The three-beam interferometer (General View)

(3) Beam-Splitter

Light from the collimator falls on a beam-splitter, B in Fig. 2, where it is split into two components going to arm (1) and arm (2) The beam-splitter used is a flat of 3 inches length, 0.44 inches thickness and 2 inches width. It has a refractive index of 1.5175 and is flat and parallel to one eight of a wave-length, the beam-splitting layer being of aluminium.

As explained in Chapter II the intensity of the third beam should be preferably equal to twice the intensity of each of the beams (1) and (2). Two-beam fringes are formed by the light beam which falls on the cube C (in Fig. 2), which consists of two prisms cemented together, with their interface semi transmitting and reflecting. Faces C_1 and C_2 (fig. 2) of the cube are fully reflecting.

The beam-splitting surface of the cube C was arranged to have approximately equal transmission and reflection, and the reflection coefficient of beam-splitter B was then arranged to have a value giving the desired intensity ratios for the different beams. Let T and R be the transmission and reflection coefficients of the beam-splitter B (Fig. 2), and T_1, R_1 be the transmission and reflection coefficients of the beam-splitter of the cube C (Fig. 2). Also let Ro be the reflection coefficient of the reflecting faces C_1, C_2 of the cube. The pentagonal prism P_1 in the arm (2) of the interferometer merely reflects the third beam, and so let Ro denote the

Plate II - Illuminating System

reflection coefficient of each of these three surfaces.

As β and α are the final amplitudes of beam (3) and of each of the beams (1) and (2) (Chapter II), they are given by

$$\beta^2 = T^2 R_o^3 \qquad (1)$$

$$\alpha^2 = R^2 T_1 R_1 R_o^2 \qquad (2)$$

From (1) and (2), the ratio of the intensity of beam (3) to that of (1) or (2) is

$$I = \frac{\beta^2}{\alpha^2} = \left(\frac{T}{R}\right)^2 \left(\frac{R_o}{R_1 T_1}\right) \qquad (3)$$

The cube beam-splitter has an aluminium film, whose transmission and reflection coefficients were found by measurement to have the values $T_1 = 32\%$ and $R_1 = 28\%$. Ro, which represents the reflection coefficient of the fully aluminised faces of the cube, was assumed to have a value equal to 95 per cent. These values for Ro, R_1 and T_1 together with the required value of $I = \frac{\beta^2}{\alpha^2} = 2$, gives for the ratio $\frac{T}{R}$, which is ratio of transmission coeffiecient to the reflection coefficent of the beam-splitter B, the optimum value of 0.44. The coating used for the beam-splitter B has the values T = 16 percent and R = 40 percent. These give very nearly the optimum value of the ratio $\frac{T}{R}$.

The beam-splitter B fits in a mount which is fixed to a very

heavy base plate, having adjusting screws for levelling. The mount of the beam-splitter also has adjusting screws, which can (a) move the beam-splitter laterally and (b) tilt it. Both these are fine motions.

The beam-splitter B divides the incoming light into two components going to the arms denoted by I and II in the diagram of the interferometer, Fig. 2. We shall discuss each of the arms I and II in turn.

(4) Arm I

Arm I of the instrument has the cube interferometer, with a right angled prism cemented to it. The light leaving the cube forms two-beam fringes, having the plane of best contrast at the reflecting faces C_1, C_2 of the cube (Fig. 2). The right angled prism which is cemented to the cube merely displaces the path of the out-coming beam laterally by a desired amount so as to let it fall at the position 'e' on the beam-splitter B(Fig. 2).

(a) The cube interferometer

The cube is formed by cementing together two right-angled prisms, cut from a single longer prism as shown in Fig 3.(a) to ensure exact equality of the adjacent angles. The glass is of refractive index 1.5175. The length of the sides is 1". The faces EF and BC Fig. 3 (b) of the prisms (1) and (2) have fully reflecting aluminium coatings. The hypotenuse, AC, has an aluminium coating

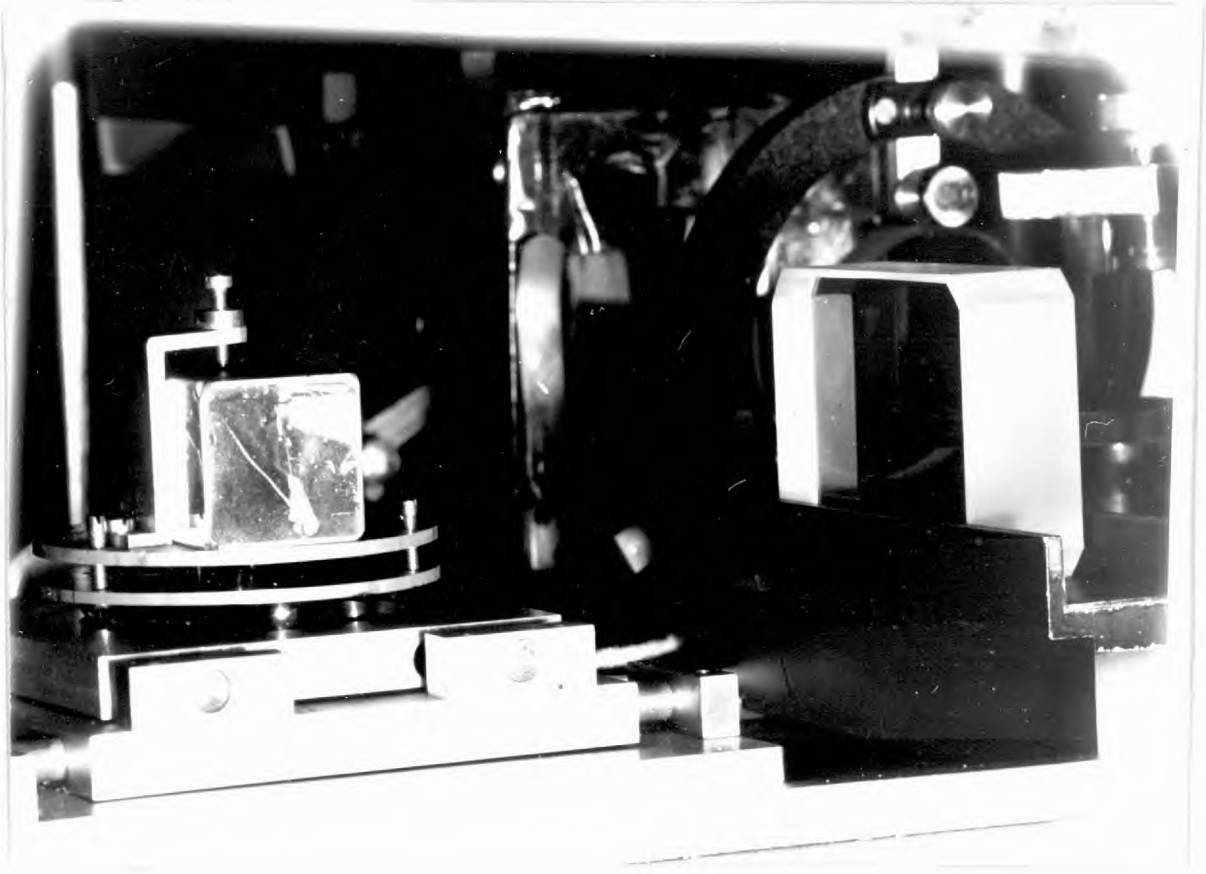

Plate III - Arm I of the interferometer

with 32 per cent transmission and 28 percent reflection. The two prisms are cemented with Bettle Resin (made by BIP Chemicals Ltd.) which has a refractive index of 1.534. The prisms are placed as shown by Fig. 3 (b), and cemented in the jig shown in Fig. 3 (c). The jig is placed in one of the arms of the Twyman interferometer, and adjustments are made to the relative positions of the two prisms until 2-beam fringes of about 70 fringes to inch are obtained. The cement used takes two days for hardening.

(b) Right Angled Prisms

The right angled prism P which is cemented to the cube C to displace the out going beam by about 1 inch, is of glass of refractive index equal to 1.5175 and sides 1 inch in length. It is cemented to the cube also using Bettle Resin. The angles of this prism are accurate to 10 seconds of arc.

This combined unit of cube and prism is placed on a mount; which, in turn, is placed on a slide to permit adjustment of the distance of the unit (cube and prism) from the beam-splitter B. The mount itself has adjustments giving both vertical and longitudinal motion in the vertical plane, and also tilt about both horizontal and vertical axes.

(5) Arm II

Light transmitted by the beam-splitter B passes along arm II of the interferometer, and a means is also provided in this arm to

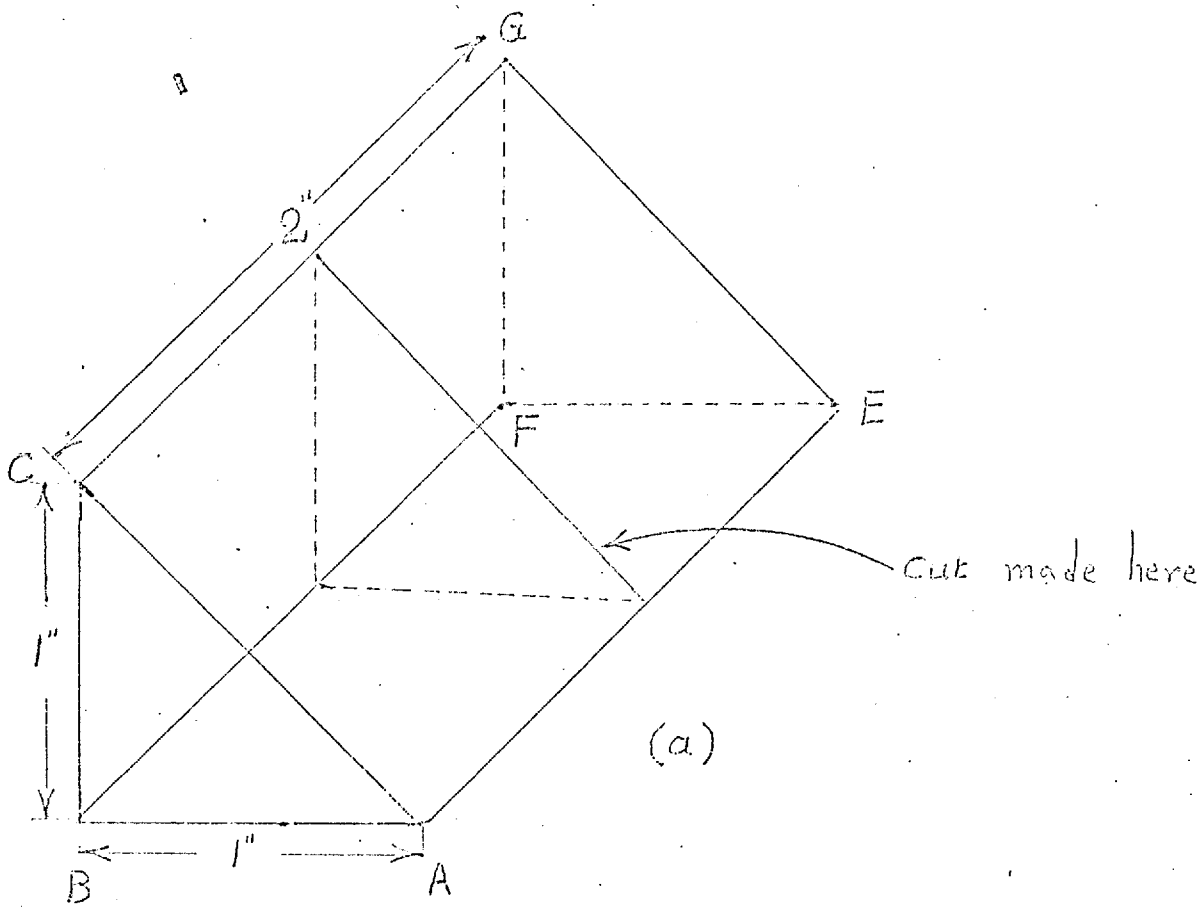

Fig. 3.

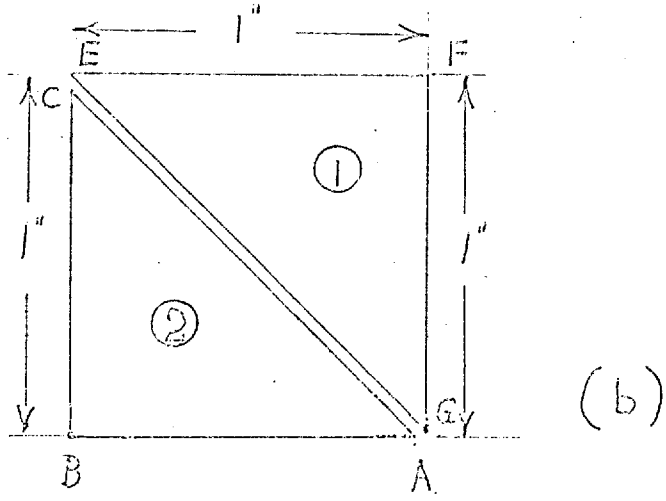

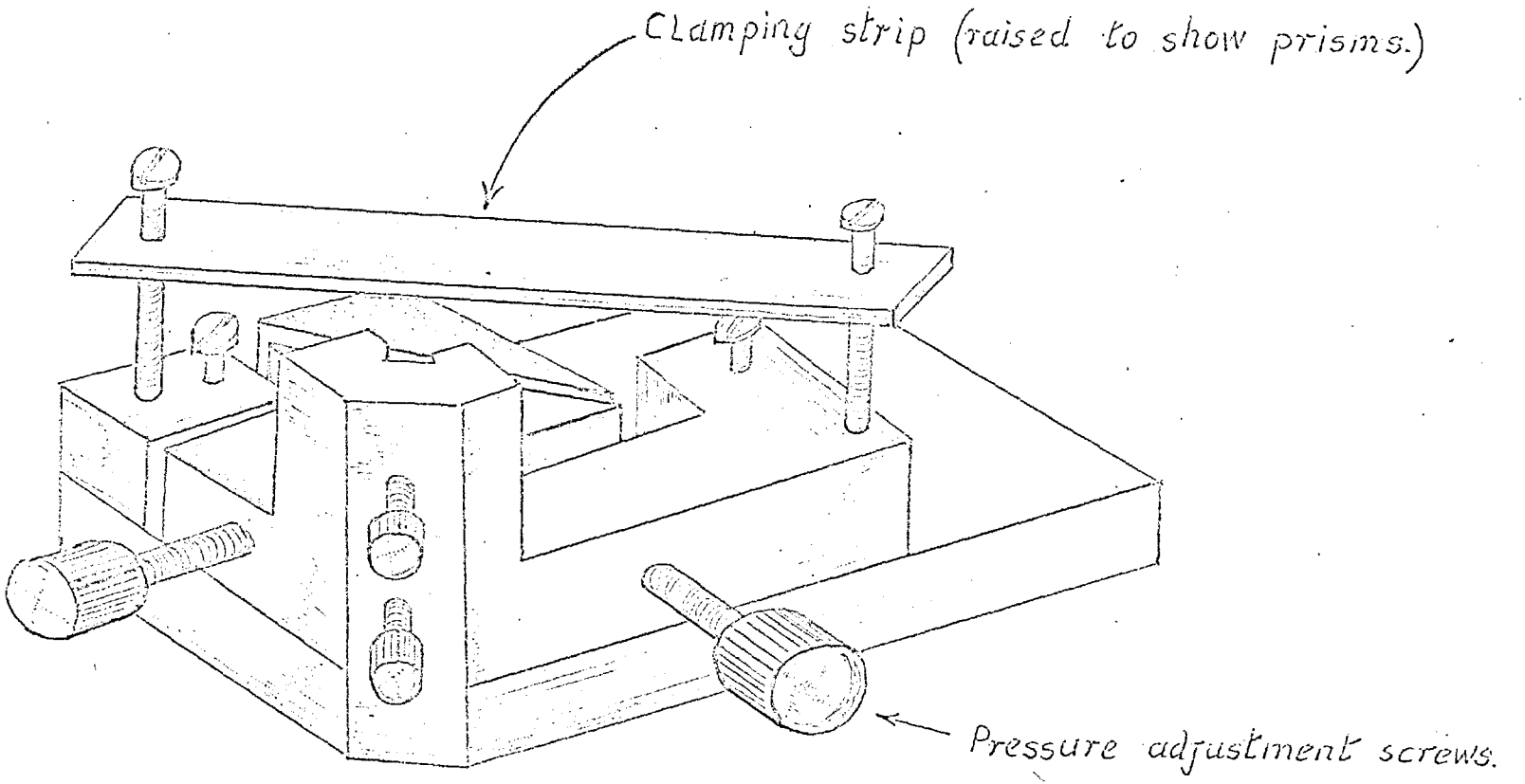

Fig. 3. (c.)

Jig for cementing prisms.

reflect the beam and displace it by the same amount as the lateral displacement of the beam in arm I, fall on the beam-splitter at the proper position. The pentaprism, P_1, is provided as well as the right angle prism P_2 in order to have three reflections in arm II as well as in arm I. This avoids relative reversal of the wave in this arm relative to the two waves reflected from the prism system in arm I. Such a relative reversal would result in poor spatial coherence between them (Chapter I), and a large reduction in the size of the pin hole would be needed to preserve fringe contrast, with a consequent large reduction in light level. The pentagonal prism has length of its sides as 1.3" and 1" and two faces P_1' and P_2' (Fig. 2). fully reflecting. The refractive index of the glass used for the pentagonal prism and for the right angled prism is 1.5175. The right angled prism has its side 1" in length. The pentagonal prism and the right angled prisms are mounted on separate mounts, which are fixed to a common base. Each prism can be given separate tilt adjustments about both horizontal and vertical axes. They can also be adjusted as a single unit in two perpendicular directions in the horizontal plane. The mount as a whole can be moved on a slide consisting of rods, and has arrangements for clamping the unit in any desired position.

Plate IV - Arm II of the interferometer

(6) The Viewing System

The right angled prism P_3 is used to reflect the beams emerging from the interferometer in a convenient direction. This prism has sides1" in length, and refractive index equal to 1.5175.

The plane of best visibility of the fringes is near to the faces C_1, C_2 of the cube interferometer C.

A plano-convex lens L_1 of 14" focal length and 4" diameter is placed at a distance of about 3" from the right angled prism P_3. Fig. 2. This forms an image of the fringes at infinity. To observe the fringes visually one has thus to place the eye at the rear focal point of L_1, where an image of the pinhole is formed.

As the spatial frequency of the two-beam fringes has to be made equal to twice the fundamental spatial frequency of the scan grating, another lens L_2 is placed after the lens L_1. L_2 is a double-convex lens with power 6 dioptres and diameter 1".

The sensitivity of the interferometer

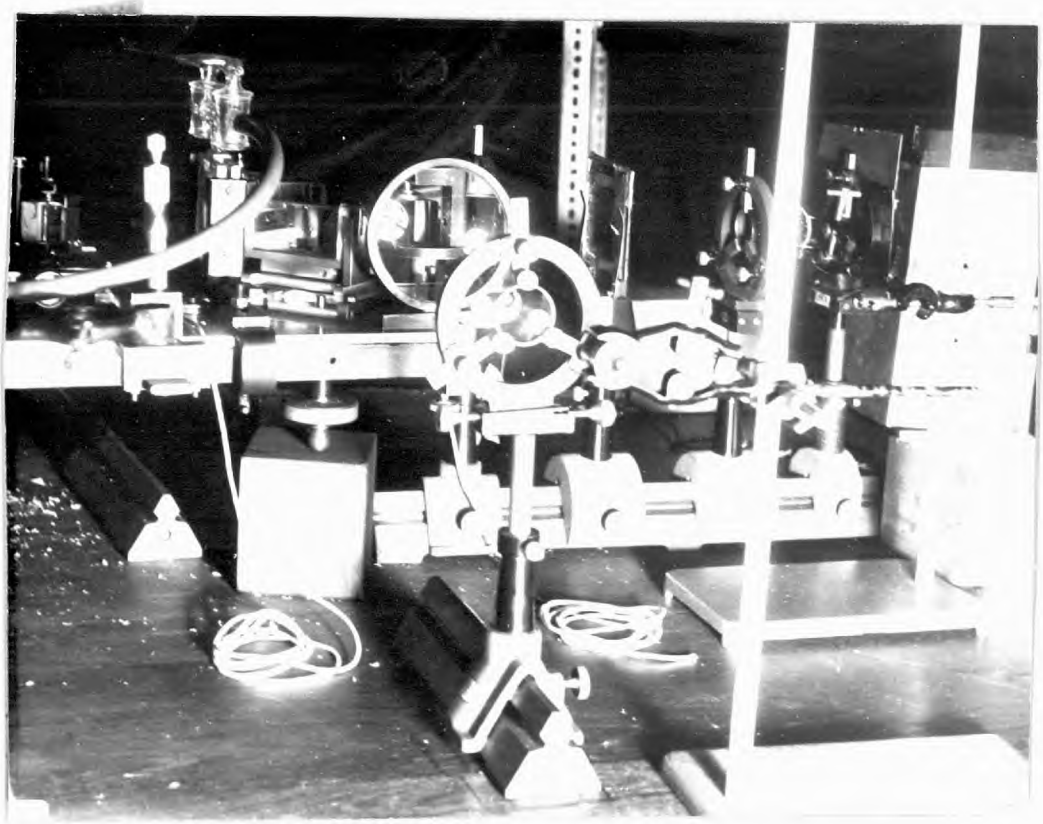

Plate V - Viewing System

may be tested by pressure scanning of air. For this purpose an air-cell is placed in the arm II of the interferometer. The air-cell is of 3 mm internal thickness, and has all faces flat and parallel to an accuracy of $\frac{\lambda}{8}$. The cell is connected to a simple manometer, which can introduce changes in pressure in air-cell of the order of 1 mm of mercury.

To make the path in glass in both the arms equal a compensator is placed in the arm I of the interferometer.

With L_1 and L_2 in position the overall magnification is not sufficient to observe easily the effect of change of pressure in the air-cell on the fringes. To facilitate visual observations we use a X10 eye-piece, which makes the total magnification of the observing system equal to about X5. With the fringes observed at a distahce of 250 mm, the fringe spacing is then equal to about 1.7 mm.

(7) Scan-grating and photo-electric detection

A scan grating placed at the position where L_1 and L_2 forms an image of the fringes. The grating is a square wave radial grating, and has a total of 1000 lines around its periphery. The mark-to-space ratio is 1:1, which is contrary to the theoretical optimum value of 0.59:1 for maximum signal to noise ratio. Simply because of immediate availability the grating with mark-to-space ratio of 1 : 1 was used.

The grating is driven at constant speed by a syhchronous motor coupled to the drum through a 1 : 6 reduction gear box. The motor is connected to the gear box by means of a rubber shaft which helps to minimise the effects of vibration. For a motor speed of 1500 r.p.m. the rate of rotation of the grating is 250 r.p.m. The A.C. carrier frequency generated is given by

$$\nu = \left(\frac{\gamma}{p}\right) c/s$$

where γ is speed (ins. sec^{-1}), and P is grating period (in),

Thus,

$$\nu = \frac{2\pi \sigma r}{60 P}$$

where σ is number of r.p.m., and r is the radius of the grating Using the values for the present instrument, namely, σ = 250 r.p.m. r = 2.1", and $P = \frac{1}{75.6}$

$$\nu = 4100 \text{ c/s}$$

for the frequency of the signals to be detected.

(8) Photomultiplier Detector

A photomultiplier is employed to convert the sinusoidally varying light fluxes into sinusoidally varying electric signals. The photomultiplier is mounted in a brass tube which is blackened on the inside. Th e photomultiplier used is an E.M.I. type 6094 B It has a spectral response as shown by Fig. 4 (a). The mercury line used in the experiment has λ = 5461 Å, for which the photo-multiplier has almost its maximum sensitivity. The 6094 B is an

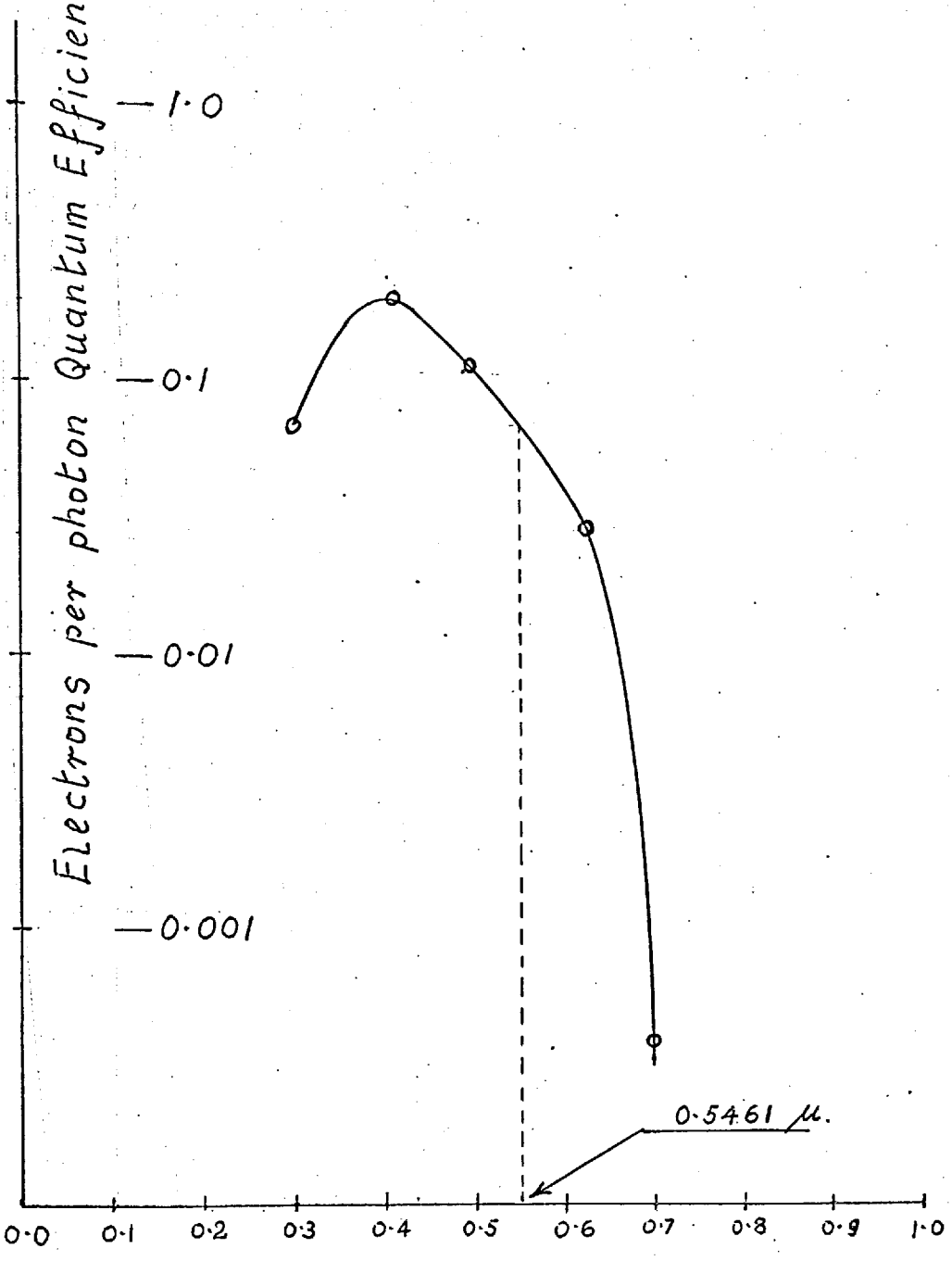

Fig. 4. (a.)

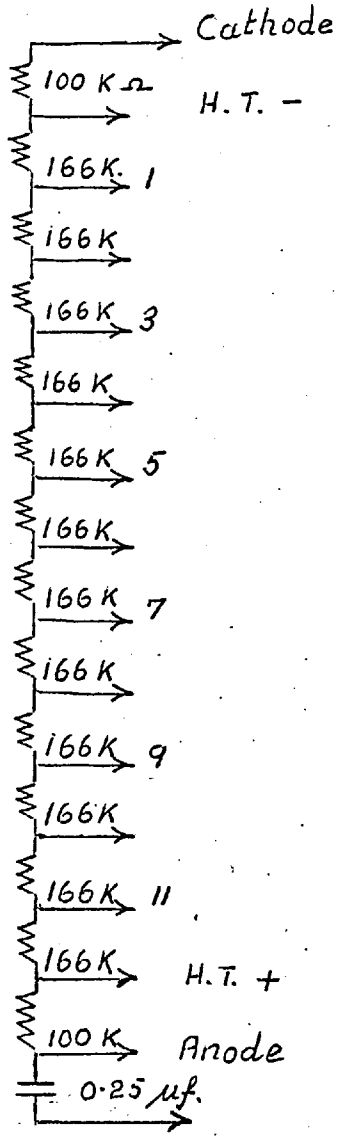

Fig. 4. (b.)

Spectral sensitivity curve for the E. M. I. Type 6094-B photomultiplier.

eleven dynode, venetian blind type tube, with a 1 centimetre diameter photocathode.

The high tension for the tube is obtained from a stabilised 2000 volt D.C. supply coupled to a potentiometer unit. Fig. 4 (b) shows the resistor chain used and connections to the photomultiplier Typical operating characteristics for the 6094 B are as follows,

E.H.T	=	1400 v
Voltage between dynodes	=	117 v
Current Drain	=	0.705 m A
Dark Current	=	3×10^{-10} A
Sensitivity	=	200 A/Lumen

Phase Selective Amplifier

The output of the photomultiplier is fed directly into an Elliott type B801 synchronous amplifier. This instrument comprises a high-gain low-noise amplifier with coarse and fine attenuation of 80 d B in steps of 20d B and 2d B, plus a smooth interpolating attenuation of 6d B at all positions. The amplifier characteristics are claimed to be stabilised throughout by negative feed-back circuits. The output is coupled to a phase sensitive rectifier which rectifies those components of the signal which are in synchronism with a reference signal which is derived from the radial grating. The reference signal is automatically controlled to a constant level

within the instrument and it can be varied cohtinuously in phase before presented to the phase sensitive rectifier.

Fig. 5. is a block diagram of the circuits incorporated within the Elliott Amplifier. Since only those parts of the signal in phase with the reference signal are rectified all signals in quadrature and at harmonics will give rise no deflection.

The Elliott Amplifier requires a sinnsoidal (or triangular) wave form of between 2 and 20 volts r.m.s. at an input impedence of approximately 10 K to 20 K for the reference channel.

Fig. 6 is a schematic diagramm of the reference channel prior to the Elliott Amplifier. The OCP 71, a junction transistor, is effectively bottomed by roughly focused light from a peanut-lamp. The output of this circuit is 15 volts RMS (as measured with a CRO) and consists of a sine-wave with slightly clipped peaks on the positive side. This appears to be suitable for the Elliott Amplifier.

Because of the extremely high sensitivity of the Elliott Amplifier, extreme care is required in separating the input channels. Input leads should always be kept short and well shielded.

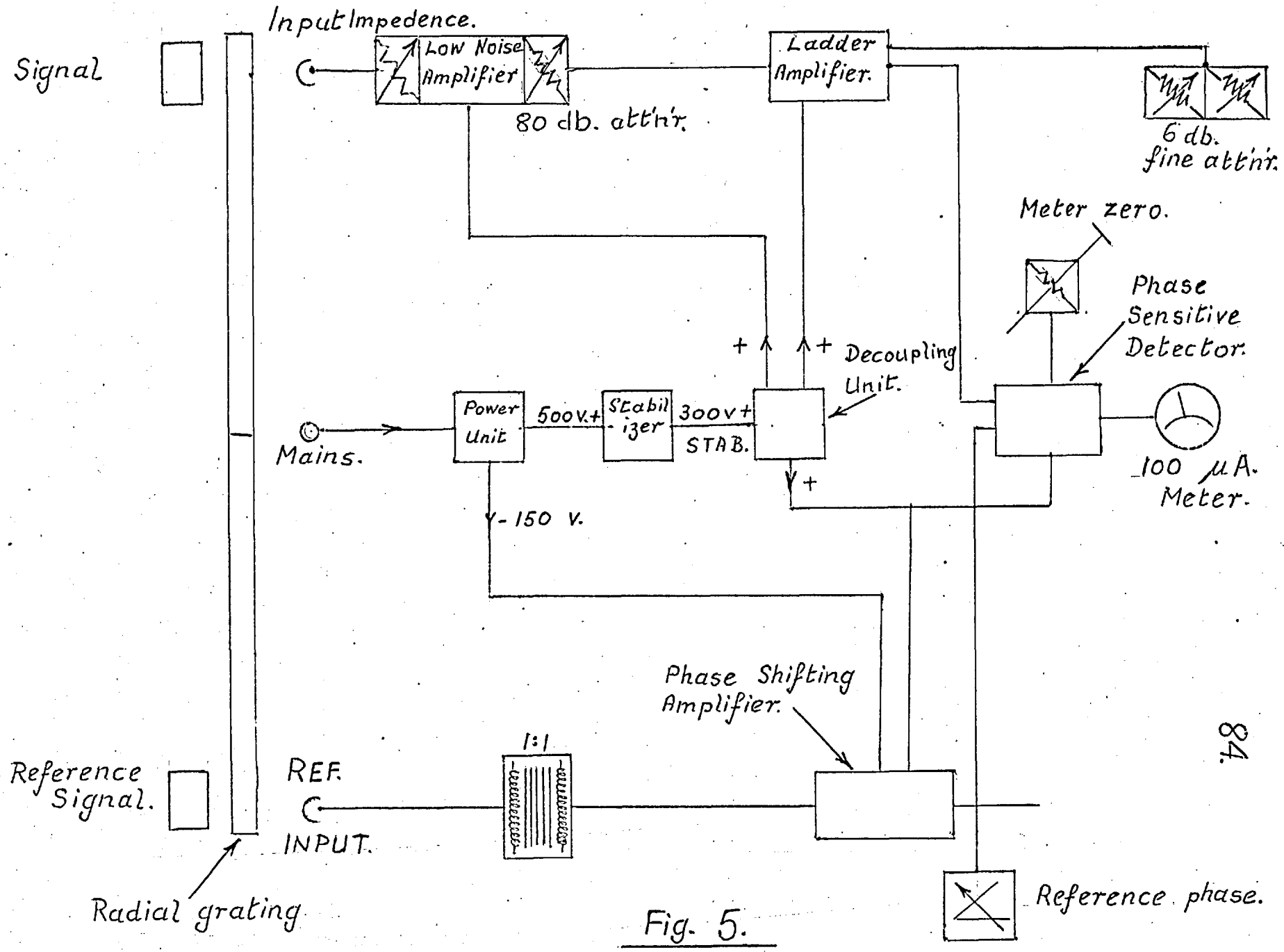
Input Impedence.
Signal
Low Noise Amplifier
80 db. attn'r.
Ladder Amplifier.
6 db. fine attn'r.
Meter zero.
Phase Sensitive Detector.
Decoupling Unit.
Power Unit
500 v.+
Stabil izer
300 v+
STAB.
Mains.
100 μA. Meter.
- 150 v.
Phase Shifting Amplifier.
1:1
Reference Signal.
REF. INPUT.
Radial grating
Reference phase.

Fig. 5.

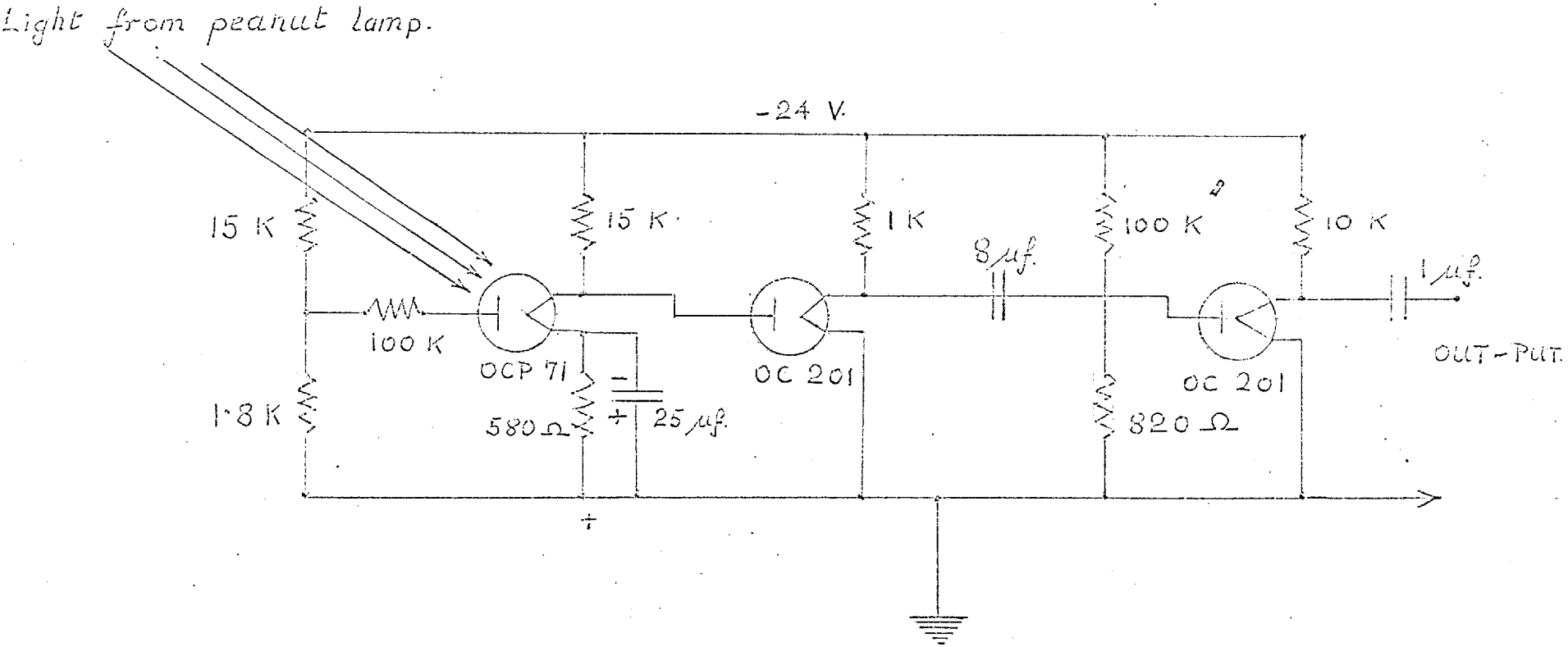
Light from peanut lamp.
-24 V.
15 K
15 K
1 K
100 K
10 K
8 µf.
1 µf.
100 K
OCP 71
OC 201
OC 201
OUT-PUT
1·8 K
580 Ω
25 µf.
820 Ω

Fig. 6.

CHAPTER VI

Adjustments of the Interferometer

Results:

A detailed description of the various components of the interferometer is given in Chapter V. The present chapter deals first with the adjustments required for observing three-beam interference.

The illuminating system of the interferometer is designed to give a uniform level of illumination in the fringes. The lenses G_1 and G_2 (in figure 2. Chapter V) form an image of the mercury lamp at iris diaphragm, which constitutes a secondary source for the interferometer. The separation between G_1 and G_2 is such that G_2 is close to the aperture in the iris diaphragm, and acts as field lens imaging the aperture of G_1 at the collimator L. It thus produces uniform illumination on the collimating lens.

The interferometer has two arms I and II. Arm I forms the two-beam fringes and arm II has the reflector of the third beam. We shall consider the adjustments of arms I and II separately.

Arm I, as mentioned earlier in Chapter V, has a cube interferometer which is mounted on a plate which has adjusting screws, which tilt the cube about two horizontal axes at right angles to each other. To obtain lateral displacements of the cube this plate

and adjusting screws are fixed to a larger plate which can be moved horizontally normal to the incident light. The whole of this assembly is carried on a further base plate which can slide parallel to the incident beam, and gives adjustment of the path length in the arm I of the interferometer.

Arm II has the reflector of the third-beam, which consists of a right angled prism and a pentagonal prism. The right angled prism receives the light transmitted by the beam-splitter B and the pentagonal prism reflects it back to the beam-splitter at the position 'e' (Fig. 2 Chapter V).

It is necessary to provide adjustments for tilting this reflector unit in order to render the wave front of the third beam parallel in the final fringes to the bisector plane of the two wave fronts returning from the cube interferometer in arm I. For this purpose the two prisms are placed on separate plates, each of which has screws which provide tilt adjustments in the horizontal and vertical planes. The prism P_2 is first adjusted laterally to superpose the reflected wave fronts on those coming from arm I. The direction of the reflected beam in arm II is then adjusted for the tilt error using the second prism, P_2'.

It was found that the adjustment initially provided for the tilt of the third beam, namely using the two screws of the prism plate, was very much too coarse to allow proper setting of the

reflector unit, and this unit of the interferometer was accordingly modified in the following manner. The plate carrying the two prisms was clamped rigidly to a beryllium-copper flexure spring which provided angular movement about a horizontal axis, and the other end of the flexure spring was attached to the main base plate through a vertical strip of beryllium-copper, providing then angular movement about a vertical axis. To obtain the fine movements needed for the adjustment of the tilt of the third beam, two levers are used with micrometer screw adjustments to provide fine motion. The initial arrangement was kept as a coarse adjustment.

Results:

With the light from arm II blocked out, 2-beam fringes were observed formed by the cube in arm I. These were photographed using a plate-holder at the fringe plane as imaged by the lenses L_1 and L_2. Figure 1 shows a photograph of these fringes. It will be noted that these fringes are not exactly straight, and this points to residual errors of surface flatness or glass inhomogeneity in the prisms forming the cube interferometer. Visually the fringes are of high contrast.

Even with the lever-operated flexure hinges it was found extremely difficult to obtain 3-beam fringes of uniform appearance.

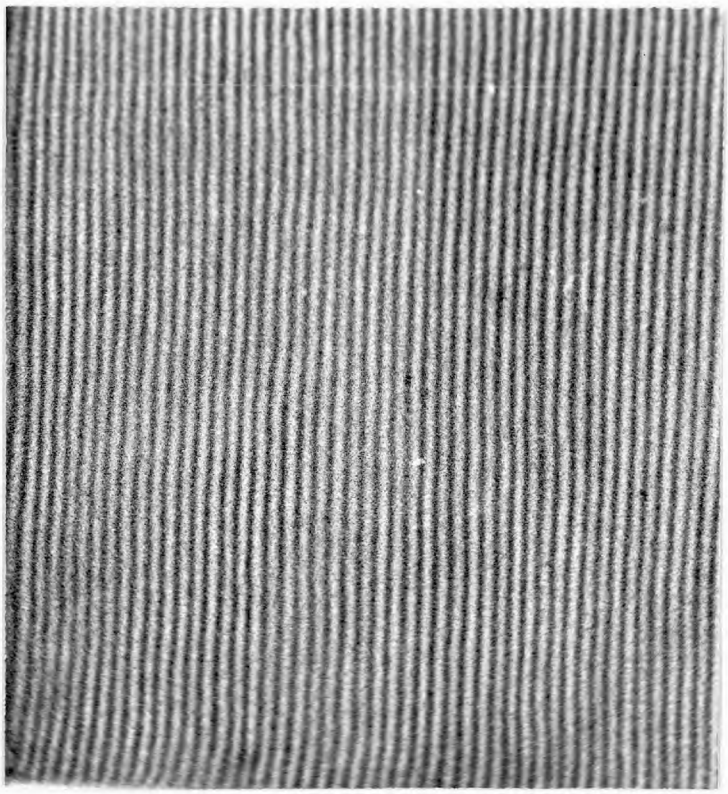

Fig. 1.

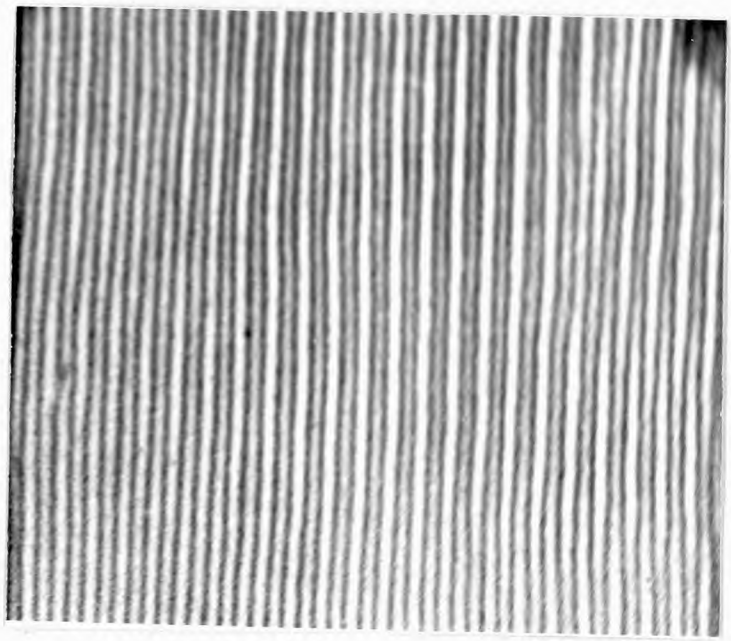

Fig. 2.

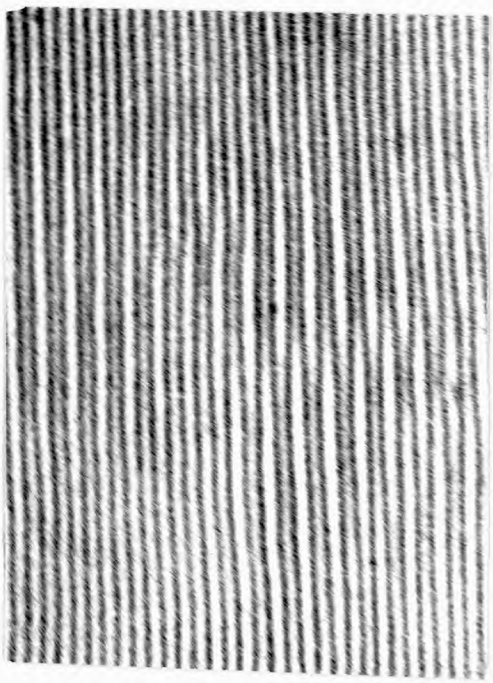

Fig. 3.

The best results obtained are shown in Fig. 2. To the middle and right of this photograph it will be seen that alternate bright fringes are of greater and less intensity, but, even here, looking along the length of fringe (from top to bottom) the relative intensity in a given fringe varies. This is seen also in moving from left to right across the centre of the fringe photograph.

The difficulty encountered arises from the extreme sensitivity of the interference effects with three beams. A very slight tilt error of the third beam will mean that the path difference between it and the light in the two-beam fringes varies from point to point over the pattern. A variation of $\lambda/100$ should be easily seen, and this would mean a precision of setting of the reflector unit, and a freedom from vibration or other movement of $\lambda/200$. Unfortunately stability of this order was not found possible with the arrangement used. The effects of residual tilt error are shown more markedly in Fig. 3, which is much more typical of the results obtained.

Given very precise adjustment of the tilt of the third beam relative to the 2-beam fringe system, the 3-beam fringes would still be very sensitive to errors of flatness of the third beam. Indeed this is so much the case that the technique might perhaps be used for the final checkings of flatness of, say, Febry-Perot

interferometer plates, where errors of the order of $\lambda/100$ can be of importance. Unfortunately, shortage of time has prevented this from being studied in practice.

Bibliography

(1) Strong, J. — Concepts of classical optics. Freeman & Company.

(2) Ditchburn, R.W. — Light. Blackie & Son Ltd. (1952)

(3) Longhurst, R.S. — Optics. Longmans Green & Co. (1957)

(4) Zernike, F. — A precision method for measuring small phase differences. J.O.S.A., Vol. 40,5,326, (1950)

(5) Vittoz, B. — Nouvelle Method de Mesure Directe de l'Effet Piezooptique, Application Au Quartz. Rev. D'-Optique Tome 35 - 1956. 253.

(6) Brown, E.B. — Modern Optics. Reinhold Publishing Corporation. (1965)

(7) Hopkins, H.H. — The Theory of Coherence and Its Applications in Advanced Optical Techniques. Editor: A.C.S. van Heel. Amsterdam: North Holland Publishing Co. (1967).

(8) Waterworth, M.D. — A New Scanning Method for the Determination of Optical Transfer Function. PhD. Thesis London University. (1966).

(9) Moss, T. — A Two-dimensional Optical Fourrier-Analyser for Image Evaluation. PhD. Thesis London University. (1964).

ACKNOWLEDGEMENTS

I wish to express my sincere thanks to Professor H.H. Hopkins for suggesting this problem and for the helpful discussions and criticisms throughout the work and for reading the manuscript.

Thanks are also due to the Government of India and the University of Delhi for giving me the study leave and to Mr. W.H. Kitchen for the help rendered in the construction of the apparatus.